Analysis of Metallothionein expression levels in mitochondrial NADH:ubiquinone oxidoreductase deficiency

Y. Olivier

Hons. B.Sc

Dissertation submitted in fulfillment of the requirements for the degree Magister Scientiae in Biochemistry at the North-West University.

Supervisor: Dr. F.H. van der Westhuizen

Co-supervisor: Prof. A. Olckers

2004

Potchefstroom

Analisering van Metallothionein uitdrukkings vlakke in mitochondriale NADH:ubiquinoon oksidoreduktase defek

Y. Olivier

Hons. B.Sc

Verhandeling ingedien vir die nakoming van die vereistes vir die graad Magister Scientiae in Biochemie aan die Noordwes-Universiteit.

Studieleier: Dr. F.H. van der Westhuizen

Medestudieleier: Prof. A. Olckers

2004

Potchefstroom

The important thing is not to stop questioning. Curiosity has its own reason for existing. One cannot help but be in awe when he contemplates the mysteries of eternity, of life, of the marvelous structure of reality. It is enough if one tries merely to comprehend a little of this mystery every day

Albert Einstein

Abstract

Some well defined functions of crucial importance for cell physiology are carried out by mitochondrial NADH:ubiquinone oxidoreductase (complex I). Deficiencies of this complex, which is one of the most frequently encountered disorders of the mitochondria, lead to multi-system disorders that includes type 2 diabetes, Parkinson's disease, Alzheimer's disease and MELAS to name only a few. The generation of reactive oxygen species (ROS) in complex I deficiency has received much attention in the last few decades. Metallothioneins (MT), which have a metal homeostasis regulating and ROS-scavenging function, were recently identified to be over expressed in complex I deficient cell lines although the cause and role of this expression remains to be investigated.

The aim of this study was to investigate metallothionein gene expression in complex I deficiency *in vitro* and evaluate related biochemical parameters, including ROS production. For this purpose, cell cultures were treated with various concentrations of an irreversible and specific complex I inhibitor, rotenone, for different incubation periods.

Results of the 24 hour incubation period indicated that with a decrease in complex I activity from 49%, the production of ROS increased approximately two fold with a 7 times increase in MT-IIA expression. Furthermore, expression of MT-IA and –IB showed baseline levels of expression, suggesting possible isoform specificity in HeLa cells. $CdCl_2$ induction showed excessive expression of MT-IIA (49 times) with almost no production of ROS, thus suggesting possible protection against ROS production. A specific ROS inducer, *t*-BHP, showed a 5 times increase in both ROS and MT-IIA expression compared to baseline levels. From our results it is evident that a complex I deficiency not only results in the production of ROS, but also the expression of MTs.

Opsomming

Sommige wel beskryfde funksies wat van groot belang is vir sel fisiologie word uitgevoer deur mitochondriale NADH:ubiquinoon oksidoreduktase (kompleks I). Defekte van hierdie kompleks lei to veelvuldige sistemiese defekte wat onder andere tipe twee diabetes, Parkinson se siekte, Alzheimeimers se siekte en MELAS, insluit. Gedurende die laaste paar dekades is baie aandag geskenk aan die generering van reaktiewe suurstof spesies (ROS) in kompleks I defekte. Metallothioniene (MT), wat 'n metaal regulerende homeostase en ROS opruimings funksie het, is onlangs in kompleks I defektiewe sel lyne verhoogde uitdrukking getoon, alhoewel die oorsaak en rol van hierdie uitdrukking nog ondersoek moet word.

Die doel van hierdie studie was om *in vitro* MT geen uitdrukking in kompleks I defekte te ondersoek, asook sommige verwante biochemiese parameters wat ROS produksie insluit. Vir hierdie ondersoek is selkulture behandel met verskillende konsentrasies van 'n onomkeerbare en spesifieke kompleks I inhibeerder (rotenoon). Verskillende inkubasie tye is ook ingelsuit by die studie.

Resultate van die 24 uur inkubasie periode dui aan dat met 'n verlaging in kompleks I aktiwiteit vanaf 49%, die produksie van ROS tweevoudig verhoog het met 'n sewe keer verhoging in MT-IIA uitdrukking. Die uitdrukking van MT-IA en –IB toon basislyn uitdrukking wat op moontlike isoform spesifisiteit in HeLa selle kan dui. $CdCl_2$ induksie toon oormatige uitdrukking van MT-IIA (49 maal) met omtrent geen ROS produksie. 'n Spesifieke ROS induseerder, *t*-BHP, toon 'n vyf maal verhoging in beide ROS en MT-IIA uitdrukking in vergelyking met basislyn vlakke. Vanuit die resultate is dit duidelik dat 'n kompleks I defek nie net aanleiding gee tot ROS produksie nie, maar ook die uitdrukking van MTs.

TABLE OF CONTENTS

LIST OF ABBREVIATIONS AND SYMBOLS

Abbreviations are listed in alphabetical order.

I	Respiratory chain complex I
1° Ab	Primary antibody
II	Respiratory chain complex II
III	Respiratory chain complex III
IV	Respiratory chain complex IV
V	Respiratory chain complex V
3D	Three dimensional
12S rRNA	12 Svedberg unit ribosomal ribonucleic acid
16S rRNA	16 Svedberg unit ribosomal ribonucleic acid

A

Å	Angstrom: 10^{-10}
α	ALPHA
ADPD	Late onset Alzheimer's disease
Ag	Silver
AIF	Apoptosis-initiating factor
ANT	Adenine nucleotide translocator
ApaF1	Apoptotic protease activating factor 1
Apo-MT	Inactive metallothionein protein
ARE	Antioxidant response elements
ATP	Adenonsine triphosphate
ADP	Adenonsine diphosphate

B

BCA	Bicinchoninic acid
Bcl2	B-cell leukaemia/lymphoma 2
Bi	Bismuth
Bp	Base pairs

BSA	Bovine Serum Albumin
β	BETA

C

cAMP	Cyclic adenosine monophosphate
cDNA	Complementary DNA
Cd	Cadmium
$CdCl_2$	Cadmium Chloride
CNS	Central nervous system
Co	Cobalt
CS	Citrate snthase
Ct	Cycle threshold
Cu	Copper
$CuSO_4.5H_2O$	Copper sulphate pentahydrate

D

Da	Dalton
H_2DCF-DA	2',7'-dichlorofluorescein diacetate
DCF	2',7'-dichlorofluorescein
DEPC	Diethyl pyrocarbonate
DMEM	Dulbecco's modified Eagle's medium
DMSO	Dimethyl sulphoxide
DNA	Deoxyribonucleic acid
dNTP	Nucleotides
dsDNA	Double strand DNA
DTNB	5,5'Dithiobis-(2-nitrobenzoic acid)

E

EDTA	Ethylenediaminetetraacetic acid
EGF	Epidermal growth factor
ELISA	Enzyme-Linked Immunosorbent Assay
et al.	And others
ETC	Electron transport chain

EtOH	Ethanol

F

FCS	Foetal calf serum
FMN	Flavin mononucleotides
FP	Flavoprotein

G

g	Gravity
GAPDH	Glyceraldehyde-3-phosphate dehydrogenase
G/C	Guanosine/cytosine
gDNA	Genomic DNA
$g.l^{-1}$	Gram per liter
GPx	Glutathione peroxidase
GRE	Glucocorticoid responce elements
GSH	Reduced glutathione
GSSG	Oxidised glutathione

H

H_2O	Water
H_2O_2	Hydrogen peroxide
Hg	Mercury
HCl	Hydrochloric acid
HP	Hydrophobic protein
hr	Hour
HRP	Horse radish peroxidase
HRSEM	High-Resolution Scanning Electron Microscopy

I

i.e.	That is
IGF-1	Insulin-like growth factor 1
IMS	Inter membrane space
IP	Iron-protein

J

Jhb	Johannesburg

K

K_2HPO_4	Dipotassium hydrophosphate
KH_2PO4	Potassium phosphate monobasic
KCN	Potassium cyanide
kDa	Kilodalton
KSS	Kearns-Sayre Syndrome

L

LHON	Leber's hereditary optic neuropathy

M

MELAS	Mitochondrial encephalopathy, lactic acidosis and stroke-like episodes
MERRF	Myoclonus epilepsy with ragged red muscle fibres
$MgCl_2$	Magnesium chloride
MIM	Mitochondrial inner membrane
Min	Minutes
MLTF	Adenomajor late transcription factor or upstream stimulatory factor.
MLV	Murine Leukemia Virus
MLV-RT	Moloney murine leukemia virus reverse transcriptase
mM	Millimolar
$mg.ml^{-1}$	milligram per milliliter
MNGIE	Myopathy and external ophthalmoplegia, neuropathy, gastro-intestinal encephalopathy
MnSOD	Manganese superoxide dismutase
MOM	Mitochondrial outer membrane
MRE	Metal responsive elements
MREa - MREg	Metal responsive elements copy a to metal responsive elements copy g

MRL	Mitochondrial research laboratory
mRNA	Messenger ribonucleic acid
MT	Metallothionein
MT-I	Metallothionein isoform type 1
MT-II	Metallothionein isoform type 2
MT-III	Metallothionein isoform type 3
MT-IV	Metallothionein isoform type 4
MT-M	Metallothionein isoform M
MT-E	Metallothionein isoform E
MtDNA	Mitochondrial DNA
MTF-1	MRE-binding transcription factor-1
MTL-5	Metallothionein like 5
mtPTP	Mitochondrial permeability transition pore
MTT	3-[4,5-Dimethylthiazol-2-yl]-2,5-diphenyl-tetrazolium bromide
µM	Micromolar
$\mu g.\mu l^{-1}$	Microgam per microliter

N

NaCl	Sodium chloride
NADH	Reduced nicotinamide adenine dinucleotide
NAD^+	Nicotinamide adenine dinucleotide
$NaHCO_3$	Sodium hydrocarbonate
NARP	Neurogenic ataxia and retinitis pigmentosa
NCBI	National center for Biotechnology information
ND	NADH:ubiquinone oxidoreductase
ND6	NADH:ubiquinone oxidoreductase subunit 6
nDNA	Nuclear DNA
Ni	Nickel
nM	Nanomolar
nm	Nanometer
NO	Nitric oxide
NRBM	National repository for biological material

O

O_2	Oxygen
$O_2^{\cdot-}$	Superoxide anion
O_H	Heavy strand origin
$OH^{\cdot}$	Hydroxyl radical
O_L	Light strand origin
$ONOO^-$	Peroxynitrite
OXPHOS	Oxidative phosphorylation

P

P	Protein concentration
P/S	Penicillin-Streptomycin
PBS	Phosphate buffer saline
PCR	Polymerase chain reaction
PEO	Progressive external ophtalmoplegia
P_H	Heavy strand promoter
P_L	Light strand promoter

R

RFU	Relative fluorescence units
ROS	Reactive oxygen species
RNA	Ribonucleic acid
rRNA	Ribosomal RNA
RSA	Republic of South Africa

S

Stdev	Standard deviation

T

t-BHP	*tert*-Butyl hydroperoxide
T*fam*	Mitochondrial transcription factor
TMB	3, 5, 3', 5' – tetramethylbenzidine
TMRM	Tetramethyrhodamine methyl ester

TNB	5-thio-2-nitrobenzoate anion
tRNA	Transfer RNA
U	
UCS	Units per citrate synthase
$U.ml^{-1}$	Units per milliliter
UV	Ultraviolet
V	
V	Volume of mitochondrial preparation
VDAC	Voltage-dependent anion channel
Z	
Zn	Zinc
$ZnCl_2$	Zinc chloride

LIST OF EQUATIONS

LIST OF FIGURES

LIST OF TABLES

ACKNOWLEGDEMENTS

The completion of the study could not have been possible without the contribution of the following people and institutions:

Dr FH van der Westhuizen, my supervisor, for the opportunity not only to participate in this project, but also for his knowledge and guidance that he imparted during the course of the year. His contribution to my scientific knowledge is greatly appreciated. Prof A Olckers, for her encouragement, advice and understanding of problems during this project.

To Oksana Levanets, for the optimisation of the real-time PCR method, as well as her commitment and willingness to help with any problems that I encountered during this year. Fimmie Reinecke, for her support and encouragement throughout this study. Leigh Cooper, for her help with the cell culture work and all the advice given during this year. To the rest of the Biochemistry department for the use of all the apparatus and opportunities given to me as post graduate student.

To Tumi Semete, for her help with the ROS production and MTT assays as well as the final stages of the optimisation of the ELISA method.

A special word of thanks to the department of Pharmacology for the use of their Bio-Rad real-time PCR machine, as well as Ann Grobler for her effort with the confocal images of our cell cultures.

A word of thanks to the NRF for the financial funding of this project.

I would like to express my eternal gratitude to my parents, family and friends for their encouragement, love and support, especially to Emma who had to deal with me during the good and bad times.

CHAPTER ONE

INTRODUCTION

Some well defined functions of crucial importance for eukaryotic cell physiology are carried out by NADH:ubiquinone oxidoreductase (complex I). This enzyme reoxidizes NADH, thus providing a certain steady state NADH/NAD^+ ratio required for continuous operation of the oxidative metabolic pathway, and it serves as the major electron entry point to the respiratory chain for further energy transduction (Grivennikova *et al.*, 2002). In humans, deficiencies of this complex is one of the most frequently encountered disorders of the mitochondria and leads to multi-system disorders that affects predominantly organs and tissues with a high energy demand like the brain, heart and skeletal muscle (Smeitink *et al.*, 2001).

In an investigation of the transcriptional response of patients with complex I deficiencies by van der Westhuizen *et al.* (2003) it was reported that a number of genes were markedly induced in complex I deficient fibroblasts. Although their investigation showed decreased mitochondrial transcripts as well as the induction of some metallothionein isoforms, some questions still remained due to the experimental setup that was required for that study. It's still not known whether metallothionein induction is reactive oxygen species (ROS) or metal induced and what the function of metallothionein expression is in complex I deficiencies.

This research project stems from the aforementioned questions. Two approaches were employed to address these objectives. The study described in this dissertation, focuses on addressing one of these questions by using an *in vitro* model for complex I deficiency. A complex I deficiency will lead to the eventual production of ROS which is postulated to induce metallothionein expression as discussed in Section 2.3.7 of the literature review chapter. The second project as described in the dissertation of Reinecke (2004), aims at elucidating the functional role of metallothionein expression in complex I deficient cell lines.

The methodology that was used in this investigation is discussed in Chapter Three. Several biochemical and molecular parameters was monitored in complex I deficient HeLa cell lines including complex I activity, metallothionein RNA and protein expression, cell viability and ROS production.

It is believed that with an induced complex I deficiency increased production of ROS will occur with the utilisation of different concentrations of a common inhibitor (rotenone). This will ultimately lead to increased metallothionein expression levels in complex I deficient cells. The results of this study are elaborated in Chapter Four, with the final conclusions and suggested future recommendations discussed in Chapter Five.

CHAPTER TWO
LITERATURE REVIEW

2.1 The Mitochondrion

2.1.1 Evolution and structure of mitochondria

The difference between prokaryotic and eukaryotic organisms is based on two characteristics. Eukaryotic cells have a genome within a membranous nuclear envelope with pores, as well as containing structures called mitochondria. The past 30 years of research have used the hypothesis of mitochondria as endosymbionts of a primitive eukaryote as illustrated by the *serial endosymbiont* theory. This theory postulates that a proto-eukariotic cell developed first, thus not containing any mitochondria (amitochondriate) and captured a proteo-bacterium through a process of endocytosis (Gray *et al.*, 1999). After a symbiotic relationship was established, genes were transfer from the bacterium to the nucleus and redundant genes were loss, thus leading to the current distribution of genes between the two genomes (Scheffler, 2001). This hypothesis was render improbable due to the vast difference between eukaryotes and prokaryotes (Voet & Voet. 1995). The current view of the mitochondria involves the fusion of an anaerobic archeobacterium (host), and a respiration-competent proteobacterium (symbiont) to form a primitive eukaryote from which all eukaryotes evolved (Scheffler, 2001).

The mitochondrion is an essential cytoplasmic organelle that provides most of the energy necessary for a cell (Morin, 2000). It is 0.5-1 μM in size and their number fluctuates between 500 to 2000 according to the specialisation and the energetic needs of the cell (Anon, 2004a; Morin, 2000). The internal structure of the mitochondria originated in the 1950's by two scientists, Palade and Sjostrand and their colleagues. The 3D architecture of multiple sectioned tissues was interpreted and two distinct membrane systems were found (Perkins & Frey, 2000). First, a

smooth and somewhat elastic outer membrane was found, term the outer membrane (MOM), and contains the voltage-dependant anion channel (VDAC) (Passarella *et al.,* 2003). The second membrane system, the inner membrane (MIM), according to Palade protrudes into the mitochondria in a "baffle-like" manner, but does not connect to the opposite periphery to form septa, as seen in Figure 2.1. The baffles form lamellae that are called cristae, as indicated in most textbooks. Sjostrand's view of the inner membrane was in contrast with Palade's. According to Sjostrand the cristae are independent lamellae (septa) with no continuity between the cristae and peripheral membranes (Figure 2.1B) (Perkins & Frey, 2000).

The development of the last decade in High-Resolution Scanning Electron Microscopy (HRSEM), electron tornography and confocal microscopy lead to the replacement of the baffle model of Palade with the cristae junction model of Sjostrand for all mitochondria (Perkins & Frey, 2000).

The intermembrane space (IMS) is included between the two membranes, and inside the inner compartment is the matrix. The matrix is a gel-liked phase which contains about 50% protein that form a reticular network that appears to be attached to the inner surface of the inner membrane (Passarella *et al.,* 2003). Furthermore, mitochondrial DNA (mtDNA) molecules, ribosomes, transfer ribonucleic acids (tRNA) and various enzymes necessary for protein synthesis, oxidation of pyruvate and fatty acids are also found in the matrix (Morin, 2000).

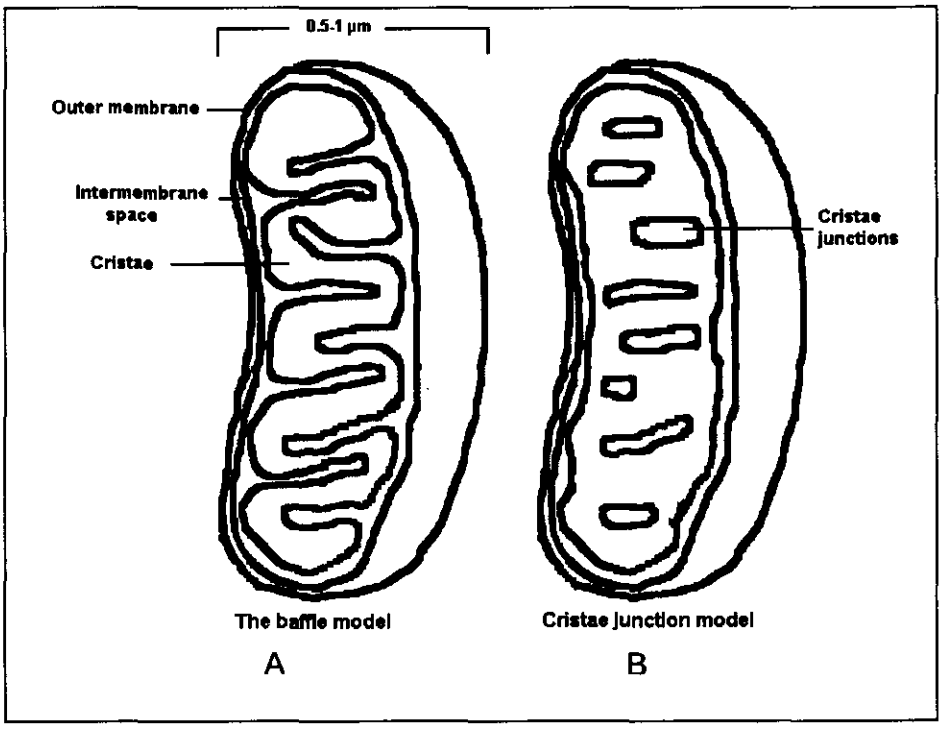

Figure 2.1: Models of mitochondrial inner membrane. The Baffle model (A) as it is commonly seen in textbooks. This model of Palade originated in 1952 and has been prominent until recently. The cristae junction model (B) that supplanted the baffle model is indicated on the right (adapted from Perkins & Frey, 2000; Oelerich, 1996).

2.1.2 Electron transport system and oxidative phosphorylation

The main function of the mitochondria is to produce energy, of which some is used for the mitochondria's own needs, and the other is transferred outside the organelle and used for various cell functions. The energy is transported out of the mitochondria by the adenine nucleotide translocator (ANT) (Smeitink *et al.*, 2001). This energy is produced by the electron transport chain (ETC) and a process called oxidative phosphorylation (OXPHOS) (Leonard & Schapira, 2000).

The electron transport chain (Figure 2.2) is under control of both the mitochondrial and nuclear genome (DiMauro, 2004). It is embedded in the lipid bilayers of the mitochondrial inner membrane, and consists of five multiprotein enzyme complexes; complex I (NADH:ubiquinone oxidoreductase) (see Section 2.2), complex II

(succinate:ubiquinone oxidoreductase), complex III (ubiquinol:cytochrome c oxidoreductase), complex IV (cytochrome c oxidoreductase) and Complex V (ATP synthase) as well as two electron carriers, the electron transfer protein coupled to ubiquinone (coenzyme Q) and cytochrome c (Anon, 2002).

Electrons, generated by the oxidation of organic acids, fatty acids and amino acids, are passed along the components of the ETC as shown by the thin black arrows in Figure 2.2. Energy are releases from the passage of electrons in the form of hydrogen ions (protons), which are pumped across the inner membrane from complex I and III and Coenzyme Q to form a proton gradient (Leonard & Schapira, 2000). This proton gradient that arise, are used by complex V to generate ATP from ADP and inorganic phosphate (Anon, 2002). This process is called oxidative phosphorylation.

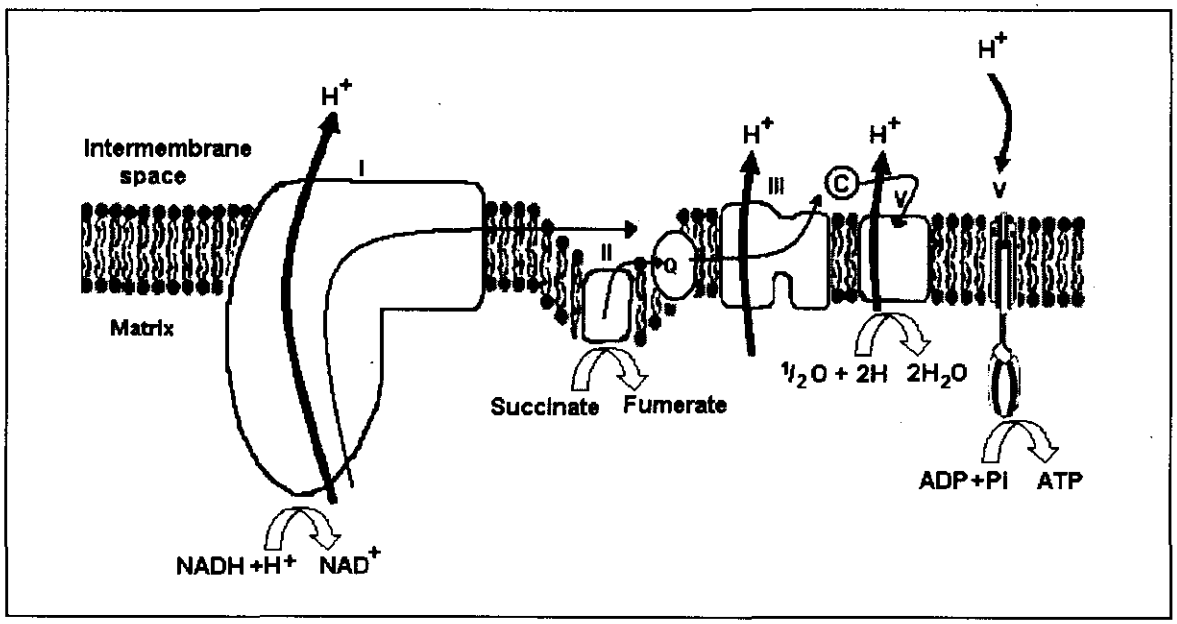

Figure 2.2: The electron transport system. This figure indicates the orientation of the complexes that forms part of the electron transport system. Complex II is situated in die mitochondrial matrix with complex I, III, IV and V in the lipid bilayers of the mitochondrial membrane. The thin black arrows indicate the flow of electrons along the chain: NADH and succinate pass electrons to complex I and II respectively. Ubiquinone shuttles these electrons to complex III. Complex III in turn reduces cytochrome c that passes electrons to complex IV. The proton gradient that arises across the inner membrane is used to generate ATP by complex V. The thick black arrows indicate the direction that H^+ are pumped to form the proton gradient (adapted from Voet & Voet, 1995).

2.1.3 Mitochondrial genome: structure and genetics

The human mitochondrial genome is a circular, double stranded molecule consisting of about 16569 base pairs (bp) (Wallace, 1999) (Figure 2.3).

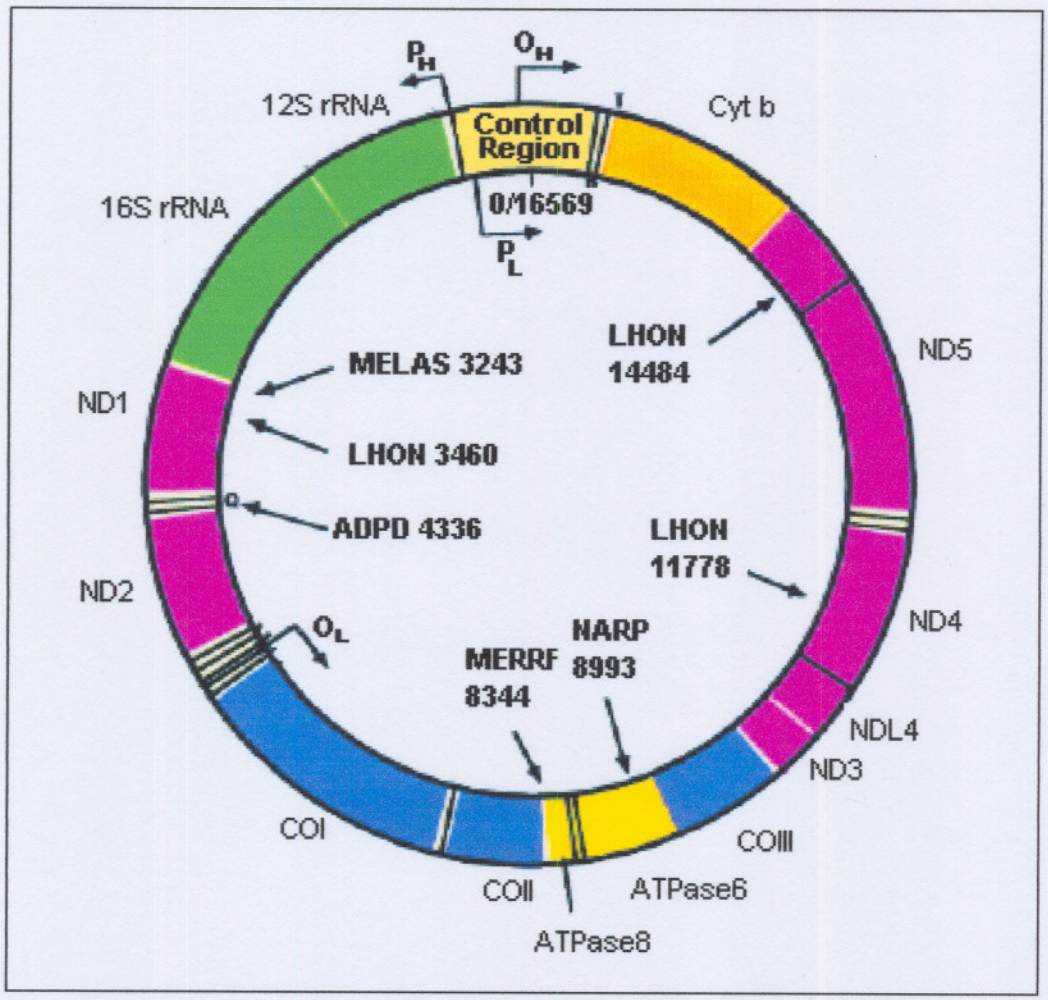

Figure 2.3: The mitochondrial genome. The human mtDNA map, showing the locations of selected pathogenic mutations within the 16569 base pare genome. Human mtDNA codes for 7 of the 46 subunits of complex I, shown in pink; one of the 11 subunits of complex III, shown in orange; three of the 13 subunits of complex IV, shown in purple; and two of 16 subunits of complex V, shown in yellow. It also codes for the small and large rRNAs, shown in green and 22 tRNAs, shown in beige. The heavy strand origin of replication (O_H) and the H-strand and light strand promoters, P_H and P_L, are indicated in the control region. The L-strand origin (O_L) is located two thirds of the way around the genome. The positions of representative pathogenic point mutations are shown on the inside of the circle, with the nucleotide position and disease acronym. All acronyms are defined in Section 2.1, except for "ADPD", which signifies late onset Alzheimer's disease (adapted from Wallace, 1999).

Ever mitochondria contains between two and ten mtDNA molecules that code 13 essential (structural) genes of ETC, two ribosomal RNAs (rRNA) and 22 tRNAs necessary for their expression (Anon, 2002). The heavy strand is the template for both the small (12S) and large (16S) rRNAs, including 12 polypeptides and 14 tRNAs. The light strand functions as a template for ND6 and eight tRNAs. All the other genes that code for mitochondrial proteins are nuclear genes (Morin, 2000).

MtDNA codes for all the subunits of the oxidative phosphorylation enzymes, except for complex II, as seen in Table 2.1 (Morin, 2000).

Table 2.1: Composition and genetic origin of OXHOS polypeptide subunits.

Complex	Subunits	Nuclear encoded	MtDNA encoded
I	46	39	7 (ND1, ND2, ND3, ND4, ND4L, ND5, ND6)
II	4	4	0
III	11	10	1 (Cytochrome b)
IV	13	10	3 (Cytochrome oxidase I, II and III)
V	12	10	2 (ATPase 6 and 8)

MtDNA coding sequences differ from nuclear genes, as it has no introns. Although the mitochondria contain several hundreds of copies of mtDNA in one cell (polyplasmy), mtDNA is still dependant on nuclear genes for some enzymes. These enzymes include those needed for replication, transcription, translation and repair. Furthermore, the mitochondria are also dependant upon the nucleus for some proteins that are involved in mitochondrial metabolic pathways (Leonard & Schapira, 2000).

In mammals, all mtDNA is inherited from the mother. Several hundred thousand mtDNAs are harboured by the female egg in contras with the few hundred mtDNAs from the sperm, resulting in the negligible effect of the sperm on the genome. However, the abovementioned "statement" has recently been debated due to the

discovery of linkage disequilibrium in human mtDNA. Mutation distribution on the heavy strand of mtDNA seems to be only attributed to one mechanism, which involves recombination between mother and father mtDNAs (Morin, 2000).

The mutation rate of human mtDNA is 10-20 times that of nuclear DNA (nDNA). This could be due to proofreading failure by mtDNA polymerases. This property, including the maternal inheritance of mtDNA is used in forensic science and the defining of ethnic populations and the plotting of their migration. Normally all mtDNA of an individual will be identical (homoplasmy), but a sequence variation can cause a population that includes wild type and mutant mtDNA (heteroplasmy) (Hauswirth & Laipis, 1982). Heteroplasmy thus implies a potentially mutant mtDNA that can result in either harmful or benign polymorphisms. The expression of these mtDNA mutations within cells and mitochondria are not only dependant on the site within the molecule but also on the proportion of the mutant to wild-type molecules (Leonard & Schapira, 2000).

The biochemical expression threshold for mtDNA mutations are about 60% compared to 95% for tRNA mutations (Chomyn *et al.*, 1991). The energy requirement of each tissue determines the degree of organ dysfunction. MtDNA mutations in the brain and muscle (which is dependent on OXPHOS), leads to common features such as neurological illnesses and myopathies. Point mutations and rearrangements (deletions and duplications) are included as mtDNA mutations but not splice-site mutations, as there are no introns. Mutations can be either maternally inherited (point mutations) or sporadic (deletions and duplications). Mitochondrial dysfunction, however, can also be due to mutations of nuclear and mitochondrial genes that are not involved with the ETC (Leonard & Schapira, 2000).

2.1.4 Mitochondrial disorders

Dysfunction of the ETC results in mitochondrial disease and are far more common than was previously realised (Chinnery, 2000). Epidemiological studies showed that the prevalence of mitochondrial disorders are at least one in 8500 which makes it most probably the most common metabolic disorder (Chinnery, 2002). The first disease associated mtDNA defect were discovered in the late 1980's and since then rearrangements (deletions and insertions) and more than 100 mtDNA point mutations have been found to be the cause of specific human diseases (Wallace *et al.*, 1988). Although mitochondrial disorders can occur at any stage, abnormalities of nDNA usually appear in childhood with mtDNA abnormalities, whether it is primary or secondary to a nuclear abnormality, occurs in late childhood or adult life (Leonard & Schapira 2000; Chinnery, 2000).

One disorder that has been associated with mitochondrial or nuclear mutations is Leigh syndrome which causes defects in every step of the OXPHOS system, but most commonly with isolated complex I or IV deficiency. Apart from Leigh syndrome, many other genetic disorders are now known to be caused by defects in the OXPHOS system. Among these are the classic mitochondrial encephalopathy, lactic asidosis and stroke-like episodes (MELAS) and myoclonus epilepsy with ragged red fibres (MERRF), as well as Leber's Hereditary Optic Neuropathy (LHON). However, because of the genetic complexity of the energy-generating system, many other diseases have been shown to have an associated defect in mitochondrial function as seen in Table 2.2 (DiMauro, 2000; DiMauro, 2003; Leonard & Schapira 2000).

Table 2.2: Disorders associated with the OXPHOS system

Complex I	Complex II	Complex III	Complex IV	Complex V
Alpers-Huttenlocher disease	Kearns-Sayre Syndrome	Cardiomyopathy	Alpers-Huttenlocher disease	LHON
Alzheimers's	Leigh's Syndrome	LHON	Deafness	Leigh's syndrome
Parkinsonism	Myopathy	Myopathy	LHON	NARP
Cardiomyopathy	Paraganglioma	PEO	Leigh's Syndrome	
Barth syndrome	Pheochromocytoma		Myopathy	
Encephalopathy			Rhabdomyolisis	
Infantile CNS			PEO	
LHON			KSS	
Leigh Syndrome			MNGIE	
Longevity			MERRF	
MELAS			MELAS	
MERRF				
PEO				

KSS, Kearns-Sayre Syndrome; LHON, Leber's hereditary optic neuropathy; MELAS, Mitochondrial encephalomyopathy, lactic acidosis and stroke-like episodes; MERRF, Myoclonic epilepsy and ragged red muscle fibers; MNGIE, Myopathy and external ophthalmoplegia, neuropathy and gastro-Intestinal encephalopathy; PEO, Progressive external ophtalmoplegia; NARP Neurogenic ataxia and retinitis pigmentosa; CNS, central nervous system (ANON, 2004c).

2.2 NADH: ubiquinone oxidoreductase (complex I)

2.2.1 Biochemistry and structure of complex I

NADH:ubiquinone oxidoreductase (EC 1.6.5.3) is the last *terra incognita* among the respiratory chain complexes. Although continuous efforts over the last five decades into the structure and function of this complex, some fundamental issues still remains unsolved. This is in contrast with the growing interest in this complex in its role in the generation of reactive oxygen species and the number of diseases that are caused by or related to complex I defects (Brandt *et al.*, 2003). Human NADH:ubiquinone oxidoreductase deficiency is one of the most frequently encountered defects of mitochondrial energy metabolism with an incidence of approximately 1:10 000 live births (Smeitink *et al.*, 2001).

Complex I is much more difficult to study than the other respiratory chain complexes for a number of reasons (Brandt *et al.*, 2003). It consists of approximately 46 different subunits of which 7 are encoded by mtDNA. The total mass is almost 980 kDA making it one of the biggest and most complicated known membrane protein complexes (Anon, 2004). No X-ray structure is so far available for this protein (Brandt *et al.*, 2003).

The function of the complex is to transfer electrons to ubiquinone (Coenzyme Q), while pumping hydrogen ions into the inter-membrane space (Grivennikova *et al.*, 1997). As mentioned in Sectioned 2.1.2, complex V uses the electrochemical proton gradient that is formed to synthesise ATP from ADP and inorganic phosphate (Smeitink *et al.*, 2004).

Complex I, which is shown in Figure 2.4, has an L-shaped structure which comprise off a water-soluble peripheral arm that partly protrudes into the mitochondrial matrix, as well as a hydrophobic arm that are embedded in the mitochondrial inner membrane (Smeitink *et al.*, 1998; Smeitink *et al.*, 2004). Flavin mononucleotides (FMN's) and iron-sulphur clusters are located in the peripheral arm (Smeitink *et al.*, 2004).

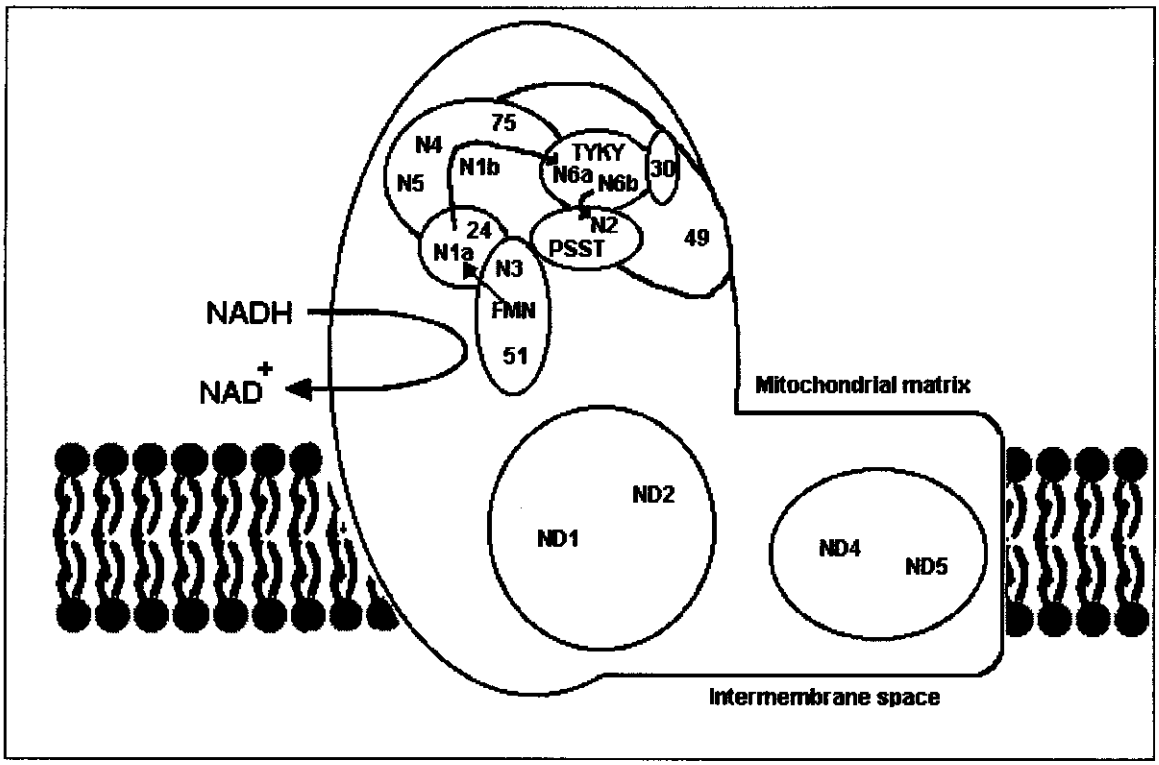

Figure 2.4: Structure of complex I. The L-shaped configuration of the complex can be seen in this figure. It consists of a hydrophobic arm and a water soluble peripheral arm which is partly embedded in the mitochondrial matrix and consists of seven highly hydrophobic subunits (ND1-ND6 and NDL4) (adapted from Brandt *et al.*, 2003).

Complex I can be separated into three different fractions with the use of chaotropic agents: the water-soluble flavoprotein (FP) and iron-protein (IP) fragments, as well as the water insoluble hydrophobic protein (HP) fragment (Smeitink *et al.*, 1998).

The principal catalytic sector are form by (1) the FP fraction that consist of a 51, 24 and 10 kDa subunit, and (2) the IP fraction, consisting of a 75, 49, 30, 18, 15 and 13 kDa and B13 subunit and is located in the peripheral arm of the complex (Belogrudov & Hatefi, 1994).

The HP fraction, containing the seven mtDNA-encoded subunits and ~24 nuclear-encoded subunits is involved in proton translocation and contains, besides hydrophobic subunits, also globular water-soluble ones (Ohnishi *et al.*, 1985; Belogrudov & Hatefi, 1994). Furthermore, the 51 kDa flavoprotein subunit carries the NADH-binding site and contains a FMN and a tetranuclear iron-sulphur cluster

(Smeitink *et al.*, 1998:1574). The 24 kDa flavoprotein subunit contains a binuclear iron-sulphur cluster and the 75-kDa iron-protein subunit contains a tetranuclear and probably also a binuclear iron-sulphur cluster (McKusick, 2003).

The iron-protein fragment contains 9 or 10 iron atoms together with a 15-kDa ubiquinone binding protein which participates in the reversible electron transfer from NADH to bulk ubiquinone coupled with the proton translocation across the mitochondrial inner membrane (McKusick, 2003).

Sequencing of the 23 kDa hydrophobic protein subunit revealed that this subunit contains two cysteine motifs which probably provide the ligands to accommodate two 4Fe-4S clusters. The flavoprotein and iron-protein water-soluble fractions make contact through the 51 kDa flavoprotein and 75 kDa iron-protein subunits (Smeitink *et al.*, 1998).

2.2.2 Inhibitors

The structure of potent natural inhibitors of complex I have a similarity to ubiquinone: a cyclic head that corresponds to the ubiquinone ring as well as a hydrophobic tail (Esposti, 1998). However, there are a number of compounds, both naturally occurring and synthetic, that are potent inhibitors of complex I. Some typical inhibitors are summarised in Table 2.3.

Rotenone (Figure 2.5) is the most potent member of the rotenoids, a family of isoflavonoids extracted from *Leguminosae* plants, and has become the classical inhibitor of complex I (Esposti, 1998).

Table 2.3: Complex I inhibitors of natural origin.

Family of compounds	Source	Potent representative
Rotonoids	Plants	Rotenone; Dequelin
Piericidins	*Streptomyces*	Piericidin A; Ubicidin-3; Hydroxypyridine
Annonaceous acetogenins	Plants	Rolliniastatin-1 or Bullatacin; Otivarin
Vanilloids	Plants	Capsaicin
Plant products	Rhubarb	Rhein
	Opium	Papaverine
Ubiquinones		Ubiquinone-2 *; Ubiquinone-3; Idebenone

(Esposti, 1998)

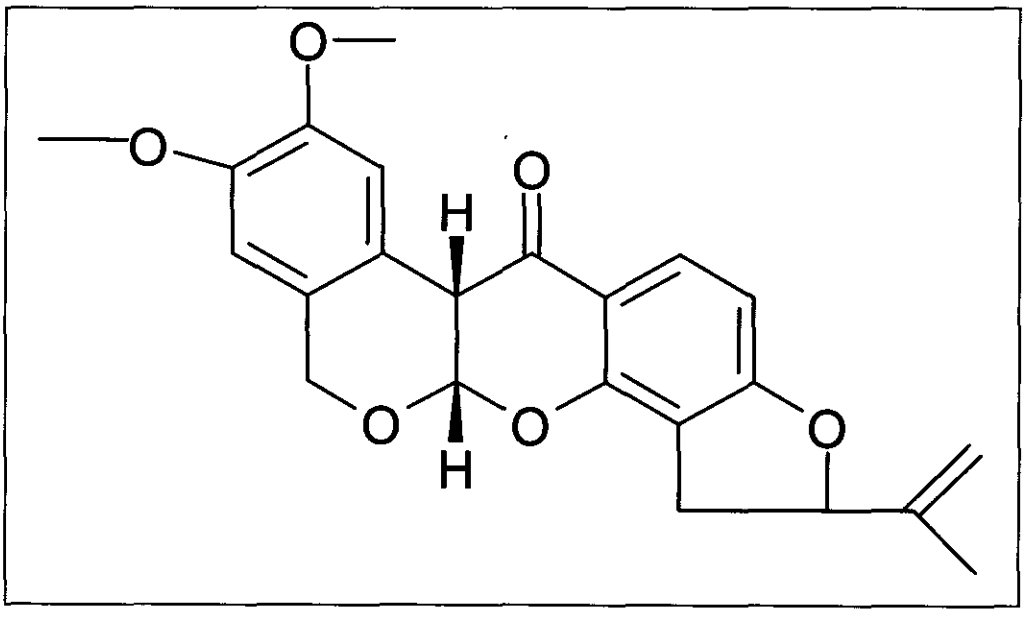

Figure 2.5: Molecular structure of rotenone (adapted from Anon, 2004b).

Rotenone is typically used to define the specific activity of complex I, and acts by inhibiting mitochondrial respiration by blocking the oxidation of NADH (Greenamyre *et al.,* 2003; Cunningham *et al.*, 1995). It is generally unstable and degrades very quickly in water, although it is more soluble in organic solvents like acetone and alcohol. Rotenone readily breaks down in the presence of light into at least 20 products, of which only 6βα,12βα-rotenolone, is toxic, making it a commonly used, naturally occurring organic pesticide (Hinson, 2000; Greenamyre *et al.,* 2003). It is extremely hydrophobic, thus meaning it can cross biological membranes easily and independently of dopamine transporters into the cytoplasm (Betarbet *et al.*, 2000). Rotenone binds irreversible and specifically to complex I, thus making it a more appropriate model candidate than other inhibitors (Greenamyre *et al.*, 2003).

2.3 ROS and Metallothioneins

2.3.1 ROS and oxidative stress

95% of all oxygen that we breathe undergoes reduction through the ETC to produce water. This reaction is catalysed by cytochrome c oxidoreductase (complex IV). Complex IV is the final acceptor and gives up its reducing equivalents to allow continued electron transport. Like any efficient system, side reaction does occur, and in the case of the ETC, side reactions occur with molecular oxygen (Cadenas & Davies, 2000). Approximately 1-3% of molecular oxygen consumed forms toxic superoxide anion ($O_2^{\cdot-}$) (Figure 2.6) (Kokoszka *et al.,* 2000), and occurs mostly at complex I and III. As indicated in Figure 2.6, superoxide anion is scavenged by mitochondrial manganese superoxide dismutase (MnSOD) to produce hydrogen peroxide (H_2O_2) (Kirkinezos & Moreas, 2001).

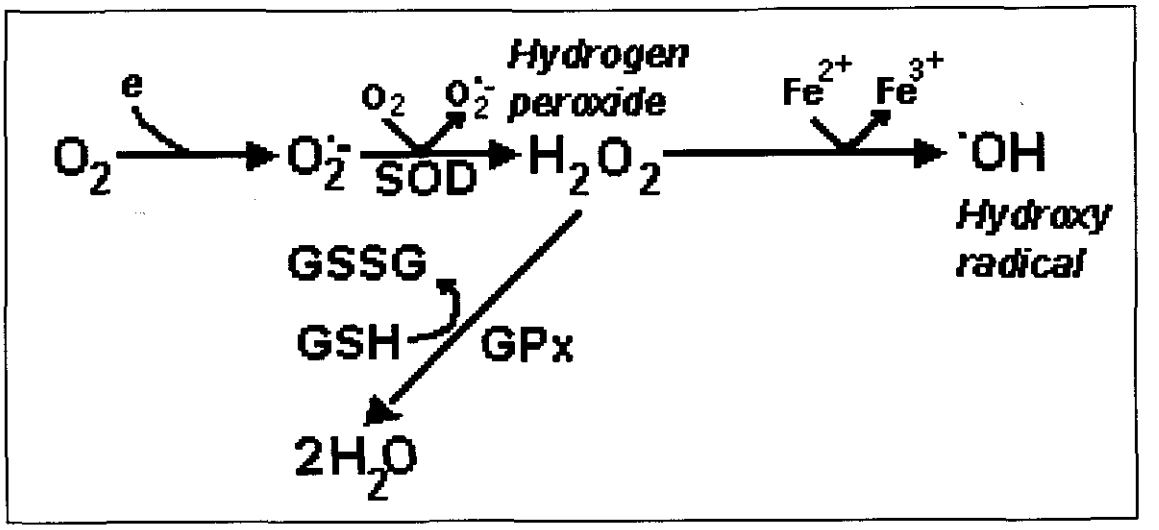

Figure 2.6: Production of reactive oxygen species. This figure indicates the formation of ROS from molecular oxygen. Superoxide anion ($O_2^{\cdot-}$) is converted to hydrogen peroxide by SOD. Hydrogen peroxide, if not broken down to water can be converted to hydroxy radicals that cause damage to lipids, membranes and ultimately to mtDNA. O_2, oxygen; GSSG, oxidised glutathione; GSH, reduced glutathione; GPx, glutathione peroxidase; H_2O, water; e, electron (adapted from Thomas, 1999).

The mitochondria's only defence against toxic hydrogen peroxide (H_2O_2) is glutathione peroxidase (GPx) since the mitochondria don't have any catalyse. H_2O_2 are converted to water by GPx in the presence of a coenzyme, reduced glutathione (GSH) and thus completely detoxifies ROS. H_2O_2 can produce the highly reactive hydroxyl radical ($OH^{\cdot}$) in the presence of transition metal through the Fenton reaction, which can cause damage to DNA, proteins, and lipids (Figure 2.7). Nitric oxide (NO) and peroxynitric ($ONOO^{\cdot}$) are two other radical species and $ONOO^{\cdot}$ can be formed in several ways, although the main source is through the reaction of NO with $O_2^{\cdot-}$(Kirkinezos & Moreas, 2001).

Normally, ROS are scavenged by a variety of antioxidants. When the level of ROS exceeds that of the antioxidants, oxidative stress occurs. The result of this imbalance between ROS that are produced and antioxidants are called oxidative stress and leads to the oxidation of several macromolecules in the mitochondria and elsewhere in the cell as shown in Figure 2.7 (Kirkinezos & Moreas, 2001).

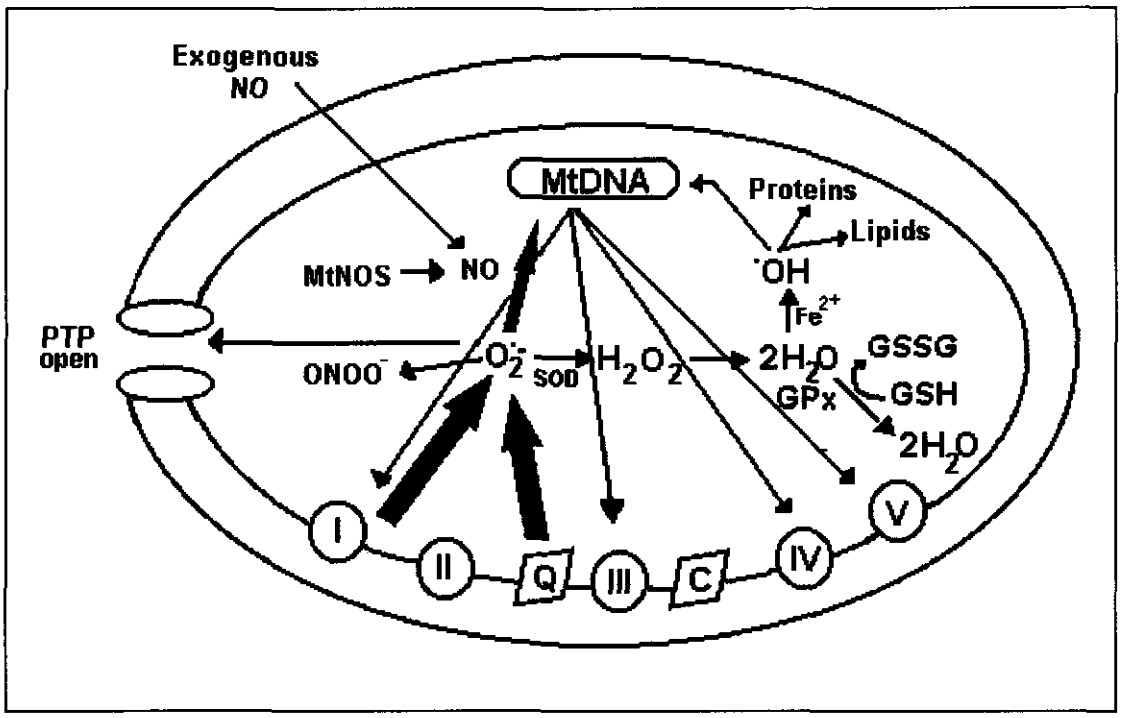

Figure 2.7: Generators and targets of ROS in mitochondria. This figure indicates the generation of the main mitochondrial ROS and their targets. The thick black arrows indicates the formation of ROS. It is clear from this figure that damage to mtDNA leads to damage of the ETC, thus forming more ROS which lead to further damage of mtDNA. PTP, permeability transition pore; GSH, reduced glutathione (modified from Kirkinezos & Moreas, 2001:450).

2.3.2 Consequences of oxidative stress

The consequences of OXPHOS defect affects multiple cellular properties, which includes alteration of the mitochondrial membrane potential, ATP/ADP ratios, ROS production and ROS-induced damage as well as mitochondrial calcium homeostasis (Smeitink *et al.*, 2001). Oxidative stress can also activate the mitochondrial permeability transition pore (mtPTP), with comprise of the inner membrane adenine nucleotide translocator, the outer membrane adenine nucleotide anion channel, Bax, Bcl2 and cyclophilin D. Activation of the mtPTP creates an open channel across the MIM and MOM, thus allowing the free diffusion of molecules between the matrix and the cytosol. The opening of the mtPTP results in the loss of membrane potential and matrix solutes and swelling of the mitochondria. The release of cytochrome c, procaspase 2, 3, and 9, apoptosis-initiating factor (AIF) and

caspase-activated DNase results in the activation of the caspase through cytochrome c and the cytosolic factor ApaF1. The caspase degrade cytosolic proteins, while AIF and caspase activated DNase the chromatin degrades in the nucleus (Kokoszka *et al.,* 2000). Furthermore, the collapsing of the membrane potential leads to the inhibition of the OXPHOS system, resulting in diminished intracellular ATP levels (Dalton *et al.*, 1999).

In addition, these events and especially the elevated ROS levels, affects transcriptional responses which contribute to the overall cell biological responses in complex I deficient cells. In a recent investigation of the transcriptional response of patients with complex I deficiencies by van der Westhuizen *et al.* (2003), it was reported that these patients have common elements in gene expression profiles, which include the induction of some metallothionein isoforms and also a decrease in mtDNA transcripts. In their investigation, the difference in genetic constitution as well as the passage numbers of cell lines required the utilisation of different controls than the commercially available clone collections. Due to this problem, van der Westhuizen and co-workers used alternative culturing conditions (glucose to galactose) to effectively challenge the oxidative metabolism in fibroblasts, thus enabling them to use the same cell lines as controls and test samples. This approach also avoided the detection of differential expression that may be due to difference in genetic constitution, age or senescence. Furthermore, it appears from their study that oxidative stress and the production of ROS play significant roles in the induction of genes that may protect against ROS itself (van der Westhuizen *et al.*, 2003).

2.3.3 General properties of metallothioneins

Metallothionein (MT) was first identified in the late 1950's as a cadmium binding protein by Margoshes and Vallee, and subsequently purified and characterised by Kagi and Vallee (Cherian *et al.*, 2003; Kagi *et al.*, 1973). These proteins are ubiquitously distributed in nature, and are characterised by its low-molecular weight (± 6,5–6,8 kDa), tetrahedral-thiolate complexes, metal thiolate clusters, and characteristic amino acid composition (Münger *et al.*, 1985; Miles *et al.*, 2000). It is a single chain polypeptide of 61 or 62 amino acid residues that contains approximately 20 cysteines, six to eight lysines, seven to ten serines, a single acetylated methionine at the amino terminus and no disulfide bonds (Hamer, 1986; Sato & Bremner, 1993; Sato & Kondoh, 2002). No aromatic amino acids, which are susceptible for oxidation, are present and also no histidines residues (Hamer, 1986)

MTs were initially classified according to the definition that they should be "polypeptides that resemble equine renal metallothionein in several of their features" (Miles *et al.*, 2000). All MTs were divided into three classes according to their structural characteristics with class I MTs defined as polypeptides with a high degree of cysteine conservation compared to those in equine kidney. Class II MTs were classified as polypeptides with less well conserved cysteine residues, thus only distantly related to equine MT and class III that included metalloisopolypeptides that contained gammaglutamyl-cysteinyl units that resembled proteinacious MTs. This classification has now been replaced by a complex but more flexible classification that classifies all MT into families, subfamilies, subgroups, and isoforms (Miles *et al.*, 2000).

2.3.4 Nomenclature and occurrence of metallothioneins

MTs are the most abundant intracellular metal binding proteins and are expressed in all eukaryotes, including plants, yeast, worms, flies and vertebrates (Andrews, 2000; Ghoshal & Jacob, 2001). In humans, metallothionein genes are clustered within the q13 region on chromosome 16 and are composed of four isoforms (Haq *et al.*, 2003). Table 2.4 summarises the different MT isoforms and is compiled from the latest publications as indicated. MT-I includes at least 13 sub-isoforms, some of which may encode RNAs that are not functional in directing production of detectable metallothionein proteins. MT-II consists of two sub-isoforms and together with MT-I is expressed ubiquitous in all tissues, including the central nervous system (except in neurons), but abundantly in fibrous and protoplasmic astrocytes (Choi, 2003). MT-III, a new member of the MT gene and protein familiy was initially identified as a growth suppressing factor of rat neuronal cells in culture, but is now expressed in the glutaminergic neurones of the brain. It is also abundant in zinc-containing neurons of the hippocampus, where it is believed to play an important role in the neuromodulation of these neurons (Haq *et al.*, 2003; Mendez-Armenta *et al.*, 2003). Literature also reported very low expression of MT-III in the pancreas and intestine, whereas the last isoform, MT-IV is expressed in the stratified squamous epithelium of the skin, tongue, and intestinal lining (Choi, 2003; Haq *et al.*, 2003; Ebadi *et al.*, 1994).

The metallothionein-like 5 gene (MTL-5, encoding tesmin protein) protein which resides on chromosome 11q13-2-q13.3 has been reported and is believe to be a marker of early male germ cell differentiation. Furthermore, through direct submission to the National Centre for Biotechnology information (NCBI) database, two additional metallothionein gene have been reported, MT-M and MT-E. Although a comparative analysis of MTL-5, MT-M and MT-E genes it has not yet been reported in the literature, the existence of these genes suggest a complex subdivision of function and expression (Haq *et al.*, 2003).

Table 2.4: Metallothionein isoforms, sub-isoforms, and expression

Isoforms	Sub-isoforms	Expression	Reference
MT-I	A	Functional	Miles *et al.*, 2000; Cherian *et al.*, 2003; Haq *et al.*, 2003
	B	Functional	Miles *et al.*, 2000; Cherian *et al.*, 2003; Haq *et al.*, 2003; van der Westhuizen *et al.*, 2003
	C	Non-Functional	Miles *et al.*, 2000
	D	Non-Functional	Miles *et al.*, 2000
	E	Functional	Miles *et al.*, 2000; Cherian *et al.*, 2003; Haq *et al.*, 2003; van der Westhuizen *et al.*, 2003
	F	Functional	Miles *et al.*, 2000; Cherian *et al.*, 2003; Haq *et al.*, 2003; van der Westhuizen *et al.*, 2003
	G	Functional	Miles *et al.*, 2000; Cherian *et al.*, 2003; Haq *et al.*, 2003; van der Westhuizen *et al.*, 2003
	H or MT-0[a]	Functional	Miles *et al.*, 2000; Cherian *et al.*, 2003; Haq *et al.*, 2003; Stennard *et al.*, 1993; van der Westhuizen *et al.*, 2003
	I	Non-Functional	Miles *et al.*, 2000; Stennard *et al.*, 1993; Haq *et al.*, 2003
	J	Non-Functional	Haq *et al.*, 2003; Miles *et al.*, 2000; Stennard *et al.*, 1993
	K	Non-Functional	Haq *et al.*, 2003; Miles *et al.*, 2000; Stennard *et al.*, 1993
	L or R[b]	Non-Functional	Haq *et al.*, 2003; Miles *et al.*, 2000; van der Westhuizen *et al.*, 2003; Stennard *et al.*, 1993
	X	Functional	Miles *et al.*, 2000; Cherian *et al.*, 2003; Haq *et al.*, 2003; Stennard *et al.*, 1993
MT-II	A	Functional	Haq *et al.*, 2003; Cherian *et al.*, 2003
	B	Non-Functional	Miles *et al.*, 2000
MT-III		Functional	Haq *et al.*, 2003; Cherian *et al.*, 2003
MT-IV		Functional	Haq *et al.*, 2003; Cherian *et al.*, 2003

[a] A putative gene that after sequencing was found to be the same as MT-IH
[b] Alias for MT-IL. (According to NCBI)

2.3.5 Structure and metal binding properties

MTs metal content is highly variable and is depended on the organism, tissue and history of heavy metal binding. For example, autopsy samples of human liver that was use to isolate MT revealed MT that contained zinc, compared to MT from kidney samples that contain both cadmium and copper (Hamer, 1986).

Metals bind to MT through thiolate bonds to all cysteine residues and can be removed by decreasing of the pH. The resulting apothionein can be reconstituted with cadmium or zinc (7 atoms) or with copper (12 atoms). Literature also reveals that mammalian MT can bind seven atoms of mercury, cobalt, lead, and nickel and/or 10-12 atoms of gold and silver (Hamer, 1986).

MTs are composed of two polynuclear clusters. The A cluster is composed of 11 cysteines which binds four atoms of zinc or cadmium or five to six atoms of copper. It is contained within the carboxy-terminal α-domain and extends from amino acids 31-61/62. The B cluster is composed of the remaining nine cysteines which can also binds four atoms of zinc or cadmium or six atoms of copper and is contained in the amino-terminal β domain that extends from amino acids 1-30 (Hamer, 1986).

The metals are tetrahedrally arranged to four cysteine thiolate ligands, with the A cluster that contains four cadmium atom binding sites. Two of these sites are bonded by three bridging sulphurs, as well as one terminal sulphur, with the remaining binding sites bonded by two bridging and two terminal sulphurs. The arrangement of the four cadmium atoms forms a distorted tetrahedron that is embedded within two overlapping six atom rings. The B cluster contains only two zinc and one cadmium binding sites. All off these binding sites are bonded by two bridging and two terminal sulphurs and the metals forms a triangle within a six atom ring that adopts a chair configuration. The metal ions form an equilateral triangle within a six atom ring that adapts a chair configuration. The metal-metal distances in the two clusters range from 3.9-5.2 Å. Both domains are globular, with diameters of 15-20 Å, and are linked by residue 30 and 31 to form a prolate ellipsoid. The protein folding patterns in the α and β domains are topologically similar but of

opposite chirality and are characterised by a high proportion of reverse turns. In both clusters, the polypeptide chain makes three turns to spiral around the metal atoms (Hamer, 1986).

2.3.6 Biological role of metallothioneins

Half a century of research and the function of MT still remains unresolved (Hamer, 1986). In attempts to determine the function of MT, different studies have been used which included:

a) animals being injected with chemicals known to induce MT
b) cells adapted to survive and grow in high concentrations of MT-inducing toxicants
c) cells transfected with the MT gene
d) MT transgenic and MT null mice (Klaasens *et al.*, 1999).

The results from these studies revealed a variety of functions for MT which includes intracellular metal metabolism and/or storage, metal donation to target apo-metalloproteins (particularly zinc finger proteins and enzymes), metal detoxification, possible protection against oxidants and free radical scavenging (Davies & Cousins, 2000). Although a range of approaches resulted in possible functions for this protein, a clear function has yet to emerge. As pointed out by Bremner (1991), it is possible that this unique protein has "some relatively basic function".

2.3.7 Induction of metallothioneins

Two of the four MT isoforms, MT-I and MT-II genes, can be induced by many types of heavy metals, oxidative stress and a wide variety of other factors as summarised in table 2.5. The induction of MTs varies with regard to the concentration and the time required of the inducing reagent (Haq *et al.*, 2003). Zinc and cadmium are as reported by Haq and co-workers (2003) the most potent inducers of transcription and protein synthesis of MT.

The transcriptional regulation by heavy metals is conferred by metal response elements (MREs) with is present on the MT promoter. These MRE has a consensus sequence, CTN**TGC(G/A)CNC**GGCCC, which is present in non-identical copies (MREa - MREg) in the 5'-flanking region of all MT genes (Haq *et al.*, 2003). MRE-binding transcription factor-1 (MTF-1), a zinc finger transcription factor in the Cys2-His2 family that have been identified in both mouse and human, binds to MREs and transactivates MT gene expression (Chu *et al.*, 1998).

For metal-inducible transcription, interaction among all the domains is required as according to activity analysis of deletion mutants of the MTF-1 gene. Metal induced MT induction requires MTF-1: if both MTF-1 alleles in embryonic stem cells are targeted, it results in the loss of basal and heavy-metal induced MT gene expression (Haq *et al.*, 2003).

Exposure of metals or stress (hypoxic or oxidative) results in the translocation of MTF-1 from the cytoplasm to the nucleus to binds to MREs on the promoter area. Gene transcription is then regulated through direct or indirect interaction with components of RNA polymerase II transcription machinery. Occupancy of the zinc fingers with zinc is required for the binding of MTF-1 to MRE (Haq *et al.*, 2003).

Table 2.5: Factors that induce metallothionein expression in cultured cells or in vivo

Metal ions	Cd, Zn, Hg, Ag, Co, Ni, Bi
Hormones and second messengers	Glucocorticoids, progesterone, estrogen, catecholamines, glucagon, angiotensin II, arginine vasopressin, adenosine, cAMP, diacylglycerol, calcium
Growth factors	Serum factors, insulin, IGF-1, EGF
Inflammatory agents and cytokines	Lipopolysaccharide, carrageenan, dextran, endotoxin, interleukin-1, interleukin-6, interferon-α, interferon-γ, tumor necrosis factor
Tumor promoters and oncogenes	Phorbol esters, *ras*.
Vitamins	Ascorbic acid, retinoate, 1α,25-Dihydroxyvitamin D_3
Antibiotics	Streptozotocin, cycloheximide, mitomycin
Cytotoxic agents	Hydrocarbons, etanol, isopropanol, formaldehyde, fatty acids, butyrate, chloroform, carbon tetrachloride, bromobenzene, iodoacetate, urethane, ethionine, di(2-ethylhexyl)phthalate, α-mercapto-β-(2-furyl)acrylate, 6-mercaptourine, diethyldithiocarbamate, penicillamine, 2,3-dimercaptopropanol, 2,3-dimercaptosuccinate, EDTA, 5-azacytidine, acetaminophen, indomethacin
Stress-producing conditions	Starvation, infection, inflammation, laparotomy, physical stress, X-irradation, high O_2 tension, ultraviolet radiation

IGF-1, Insulin-like growth factor 1; EGF, epidermal growth factor; Cd, cadmium; Zn, zinc; Hg, mercury; Co, cobalt; Ni, nickel; Bi, bismuth; cAMP, cyclic adenosine monphosphate. (Kagi, 1991)

As indicated in Table 2.5, a variety of metals can induce MT and therefore also the activity of MTF-1, but only zinc can mediate binding to DNA. Therefore is MTF-1 directly responsive only to zinc, which suggest that zinc may activate the protein by allosteric interaction. Figure 2.8 illustrates a proposed model which suggests that zinc can be displaced from intra and/or extra-cellular storage proteins by inducing non-zinc heavy metal concentrations, thus increasing the free zinc pool that are available for the activation of MTF-1 through binding to MTF-1. MTF-1 DNA binding activity thus increase as a result of zinc induction and this correlates with an increased in MT transcription (Haq *et al*, 2003).

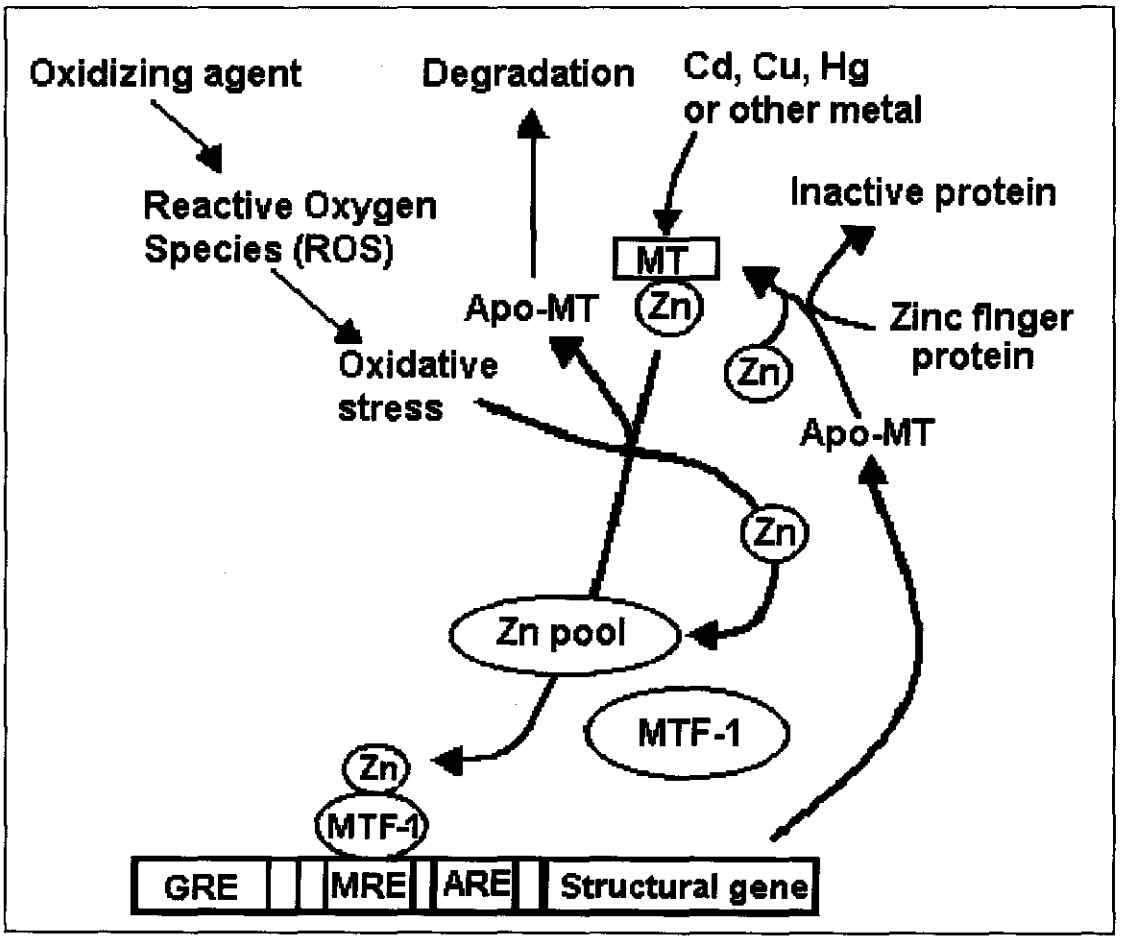

Figure 2.8: A model for induction of metallothionein gene expression. Non-zinc heavy metals displace zinc from storage proteins, thus increasing zinc pool for activation of MTF-1. MTF-1 binds to zinc after which binding to MRE occurs. It is believed that MT scavenges ROS (due to oxidative stress) by forming disulfide bonds with cysteine residues resulting in the displacement of zinc that enters the zinc pool. Due to the displacement of zinc from MT, an Apo-MT forms that subsequently disassembles (adapted from Haq *et al.*, 2003; Sato & Kondoh, 2002).

Although the precise mechanism by which inducing agents activate MTF-1 is not resolved, it is recognized that MTF-1 is a critical transcription factor that regulates inducing of MT gene expression. One possible mechanism is that the activity of MTF-1 could possible depends on a metalloregulatory proteins that do not contain DNA binding or trans-activation capacities. Zinc would be added from MTF-1 as a respond to inducing events by such a "regulator". MTs are single ligand species that release zinc in response to induction with cadmium and zinc or exposure to ROS, thus making them ideal candidates for the role, and the released zinc would then be available for MTF-1 activation as described on the previous page (p27) (Haq *et al.*, 2000).

2.4 Problem statement, Hypothesis, Aims of the study

2.4.1 Problem statement

There is a growing awareness that oxidative stress plays a role in various clinical conditions such as diabetes type II, HIV infections, cardiovascular diseases, neurodegenerative disease and many more. An understanding of the consequence of mitochondrial related oxidative stress is still not yet clear, and is crucial to understand the mechanisms that lead to the pathologies of these diseases. One of the responses, as reported by van der Westhuizen *et al.* (2003) and discussed in Sectioned 2.3.2, is the induction of several isoforms of metallothioneins in complex I deficient fibroblast cell lines.

Although the study by van der Westhuizen and co-workers were performed on patient fibroblasts with proven complex I deficiencies under a specific experimental setup, the induction of MTs in complex I deficiency still needs to be investigated further. This includes the question of the role of these proteins and if their induction is ROS or metal related. It is known that with a complex I deficiency, overproduction of ROS occurs and it is believed that ROS is scavenged, not only through antioxidants, but also through the induction of metallothioneins. It is therefore hypothesised here that a complex I deficiency will result in the induction of metallothionein gene expression.

2.4.2 Aims of study

The aim of this study was to investigate the induction of metallothionein gene expression in a complex I deficiency. Specific aims include:

- Induction of a complex I deficiency in cultured cells with rotenone at different concentrations and incubation times.
- Analysis of biochemical parameters associated with a complex I deficiency.
- Investigation of metallothionein expression on RNA and protein level in the induced complex I deficient cells.

2.4.3 Strategy

To accomplish the aims of this investigation, the following strategy has been drafted, as outlined below in Figure 2.9.

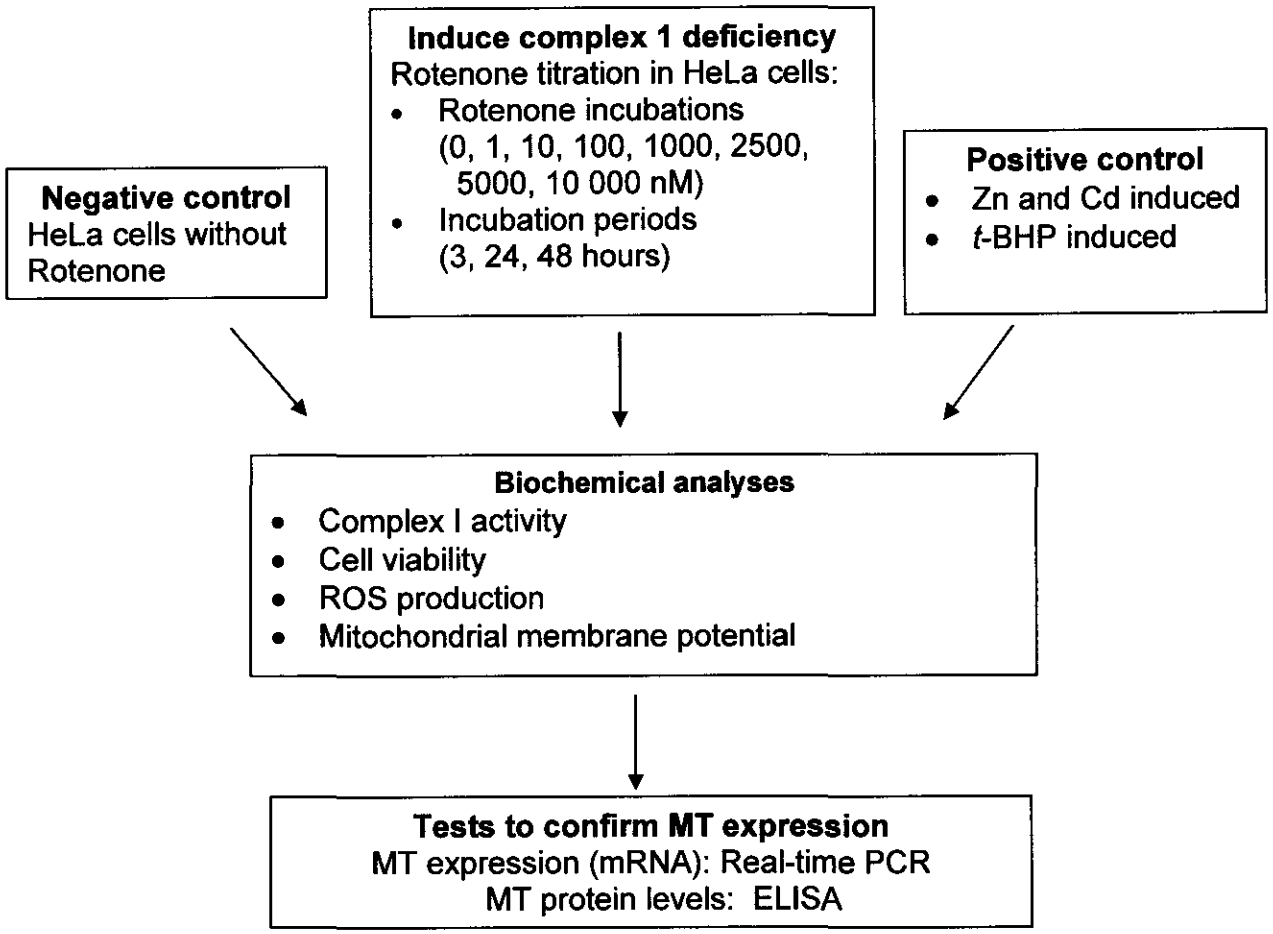

Figure 2.9: Flow diagram detailing the experimental layout of this investigation

HeLa cells, a malignant cell line from the cervix of Henrietta Lacks, were chosen to use in this study for numerous reasons. During the last 45 years of research on HeLa cells, a great deal about the physiology and genetics of these cells are known and their ability to grow very aggressively in culture made them the best

experimental model for this *in vivo* study. Importantly, for relevance to mitochondrial research, the mtDNA sequence of HeLa cells is known, in fact it was the first to be sequenced. Furthermore, several *in vivo* studies on MT expression and induction have been performed using HeLa cells (Karin & Herchmann, 1981; Koizumi *et al.*, 1985; Zhang *et al.*, 2003).

As discussed in Section 2.2.2, rotenone was used to induce a complex I deficiency. Different concentrations and incubation times were utilised to determine the effect of ROS production via rotenone on the expression of MT. Cadmium and zinc were use as controls for metal induction on MT expression.

MT expression was analysed on RNA and protein level by real-time PCR and enzyme linked immunosorbent assays. These and other biochemical analyses will be discussed in detail in Chapter Three.

CHAPTER THREE

EXPERIMENTAL PROCEDURES

3.1 Introduction

Many of the experimental methods used in this investigation are standard assays of the Mitochondrial Research Laboratory (MRL) at the Biochemistry Division of the School for Chemistry and Biochemistry, North-West University, Potchefstroom campus. These methods include cell viability test via the use of MTT, complex I activity analysis, citrate synthase activity and protein determination. Four methods, however, real-time PCR, ELISA, ROS production and mitochondrial membrane potential analyses, had to be standardised. The analyses were performed *in vitro*. The choice of the methods used for these four assays was based on the detection limits required, availability of equipment and financial considerations.

3.2 Cell Cultures

HeLa cells obtained from the National Repository for Biological Material (NRBM) were used for this investigation. These cells were grown in 25 cm^2 Nunclon flasks in Dulbecco's modified Eagle's medium (DMEM, Highveld Biologicals, Jhb, RSA), supplemented with 4.5 $g.l^{-1}$ glucose and 0.110 $g.l^{-1}$ sodium pyruvate with L-glutamate, 5% foetal calf serum (FCS, GIBCO™[1]) and penicillin (250 $U.ml^{-1}$, GIBCO™) and streptomycin (250 $\mu g.ml^{-1}$, GIBCO™). Flasks were placed in a humidified HERA cell incubator (Kendro Laboratory Products) at 37 °C with 5% CO_2.

[1] GIBCO™ is a trade mark of Invitrogen Corporation, Grand Island, NY, USA.

3.2.1 Cell treatment

Cell cultures at approximate densities of 70 - 90%, were initially treated with 1, 10, 100, 1000, 2500, 5000, and 10 000 nM of rotenone (Sigma-aldrich) respectively, and incubated for 24 hrs. A rotenone stock solution of 750 μM, dissolved in ethanol (EtOH) was used for the incubations. A control cell culture received the same volume of EtOH as the rotenone treated cells and was included in the initial and main study to serve as negative control. A subset of control cell cultures were treated with 12.5 μM cadmium chloride ($CdCl_2$, Merck) and 250 μM zinc chloride ($ZnCl_2$, Merck) and included in the 24 and 48 hour induction periods to serve as positive controls for the induction of metallothionein expression. A second positive control that was included in the 3 hour induction period was treated with 0.5-, 0.8-, and 1 mM of *tert*-butyl hydroperoxide (*t*-BHP, Sigma-aldrich) respectively.

3.2.2 Harvesting of cells after induction

After the induction period, cells were trypsinated according to standard cell culture procedures of the MRL. The trypsinated cells were suspended in 10 ml of phosphate buffer saline (PBS, BioWhittaker™[1]) containing NaCl, K_2HPO_4 and KH_2PO_4 and transferred to a 10 ml conical tube before centrifugation (600 times gravitational force (x g), 5 min). The supernatant was discarded and the pellet resuspended in 1 ml of PBS and transferred to a microcentrifuge tube.

3.3 OXPHOS analyses

3.3.1 Isolation of mitochondria

Enriched mitochondrial preparations from rotenone-induced HeLa cells, prepared by differential centrifugation, were used for the enzymatic analyses. Cells were

[1] BioWhittaker™ is a trademark of Cambrex Bioscience Inc, MD, USA

harvested from 185 cm^2 Nunclon flasks as described in Section 3.2.2, and resuspended in three ml of a sucrose, EDTA and Tris (SET) buffer (0.25 M sucrose, 2 mM EDTA, 10 mM Tris, pH 7.4) on ice. The homogenate was prepared using 15 strokes in a tight-fitting Potter-Elvehjam homogeniser that was kept in ice water. The homogenate was transferred into a microcentrifuge tube and centrifuged at 600 x g for 10 min at 4°C. The supernatant was transferred to a new tube and centrifuge at 10 000 x g for 10 min at 4°C. The supernatant was discarded. The mitochondria-enriched pellet was washed with 500 µl Hypotonic buffer (0.5 M KH_2PO_4, 0.5 M K_2HPO_4, 1 M $MgCl_2$, pH 7.2) and centrifuged at 600 x g for 5 min at 4°C. The pellet was resuspended in 200 µl of Hypotonic buffer and stored at –70°C until the assay were performed. Before enzymatic analyses, tubes containing the mitochondrial pellets were thawed on ice. Samples were frozen and thawed two more times and then sonicated (MSE soniprep 150) briefly for three seconds, with the tube placed in ice water, to assist thorough mixing of the sample.

3.3.2 NADH:ubiquinone oxidoreductase assay (complex I)

The activity of NADH:ubiquinone oxidoreductase can be measured spectrophotometric by either measuring the oxidation of NADH or the reduction of ubiquinone analogues or homologues. The assay used in this study was based on the oxidation of NADH at 340 nm. Electrons passing through active complex I enzymes are forced to coenzyme Q1, which participates as an alternative electron receiver and by inhibiting complex III with KCN (Trounce *et al.*, 1996).

Complex I activity was measured using the mitochondrial-enriched pellet homogenates according to the conditions describe by Rahman *et al.* (1996). To measure the activity, 20 µl of mitochondrial preparation was mixed with 472.5 µl of milliQ water in a quartz cuvette. Subsequent to a three min incubation to assist hypotonic lysis, 2.5 µl of coenzyme Q1 (10mM in EtOH, Sigma-aldrich), 5 µl of EtOH and 87.5 µl of assay reagent was added. The assay reagent was composed of a potassium buffer (0.5M KH_2PO_4, 0.5M K_2HPO4, pH 7.4), NADH (2 mM), KCN (50 mM), antimycin (0.5 mM) and BSA (1 $mg.ml^{-1}$). NADH oxidation was measured

at 340 nm on a BIO-TEK Uvikon UV-Vis double beam spectrophotometer in 1 min intervals for 10 min (A1). Each sample volume was assayed in two separate cuvettes, one of which contains 5 µl of 0.75 mM rotenone (A2) rather than 5 µl of EtOH which enable the estimation of rotenone-sensitive complex I activity. The activity of complex I was calculated using Equation 3.1 and was finally normalised against citrate synthase activity using Equation 3.2.

Equation 3.1: NADH:ubiquinone oxidoreductase activity

$$\text{Activity} = [(A1 - A2) / 6.81^*) / ((v/1000)^*P)] \times 0.05$$
$$= \text{nmole.min}^{-1}\text{.mg}^{-1}$$

*Extintion coefficient for NADH (340nm) which includes correction of the contribution of CoQ1 at 340nm = 6.81 $mM^{-1}.cm^{-1}$; A1 = absorbance of sample that contains 5 µl of EtOH; A2 = absorbance of sample that contains 5 µl of rotenone; v = volume (µl) mitochondrial preparation; P = protein concentration ($mg.ml^{-1}$).

Equation 3.2: Normalisation of complex I activity against citrate synthase activity

$$\text{Complex I activity} = \text{complex I activity}^* / \text{CS activity}^*$$
$$= \text{nmole.min}^{-1}\text{.UCS}$$

*Expressed as $nmol.min^{-1}.mg^{-1}$ UCS, units citrate synthase ($\mu mole.min^{-1}$).

3.3.3 Combined complex I + III assay

Owing to high levels of rotenone-insensitive activities that were detected in mitochondrial pellets, combined complex I + III activity was also measured in enriched mitochondrial pellets. The NADH-dependent reduction of cytochrome c is followed at 550 nm as described before (Trounce *et al.*, 1996).

To measure the activity, 10 µl of the mitochondrial preparation was mixed with 368 µl of milliQ water preheated to 37 °C.in a cuvette. Subsequent to a 3 min incubation, 100 µl of Medium F (5 $mg.ml^{-1}$ BSA, 50 mM Tris-HCl, pH 8.0), 10 µl cytochrome c (2 mM) and 10 µl NADH (0.8 mM) was added. The reaction rate

was measured at 550 nm on a BIO-TEK Uvikon UV-Vis double beam spectrophotometer for 2 min (A1). In a parallel cuvette reaction, rotenone was added to a final concentration of 3 μM and the rate recorded at 550 nm for 2 min (A2). The activity ($\mu mole.min^{-1}.mg^{-1}$) was calculated according to Equation 3.3. Combined complex I + III (rotenone sensitive) activity was finally normalised against citrate synthase activity as described in Equation 3.2

Equation 3.3: Combined complex I + III activity calculation

$$\text{Activity} = [(A1-A2)/29.5^*)/ (0.01 \text{ ml} \times P]$$
$$= \text{nmole.min}^{-1}.\text{mg}^{-1}$$

*Extinction coefficient for cytochrome c = 29.5 $mM^{-1}.cm^{-1}$; A1 = rate of cytochrome c oxidation with rotenone excluding; A2 = rate of cytochrome c oxidation with rotenone included; P = protein concentration ($mg.ml^{-1}$).

3.3.4 Ubiquinol:cytochrome c oxidoreductase (complex III assay)

The following assay monitors the reduction of cytochrome c at 550 nm catalysed by complex III in the presence of reduced decylubiquinone (Trounce *et al.*, 1996).

To measure the activity, 90 μl of assay reagent was mixed with 353 μl of milliQ water in a disposable cuvette. The assay reagent was composed of a potassium buffer (0.5 M), n-dodecylmaltoside (25 mM), KCN (50 mM), rotenone (0.25 mM) and BSA (1 $mg.ml^{-1}$). Subsequent to a 5-10 min incubation at 30 °C, 10 μl of sample and 5 μl of reduced decylubiquinone was added. The reaction was started with the addition of 4 μl of cytochrome c (2 mM) and spectrophotometric readings at 550 nm were recorded for 10 min (A1) on a BIO-TEK Uvikon UV-Vis double beam spectrophotometer. Each sample volume was assayed in two separate cuvettes, one of which contained H_2O (A2) instead of 10 μl sample. The activity was calculated as describe for complex I + III using Equation 3.3 and normalised to citrate synthase as described in Equation 3.2.

3.4 Citrate synthase activity

Citrate synthase is the most commonly used mitochondrial matrix marker enzyme and is a common inclusion in OXPHOS studies. This assay follows the reduction of 5,5'dithiobis-(2-nitrobenzoic acid) (DTNB) at 412 nm which is coupled to the reduction of acetyl-CoA by the citrate synthase reaction in the presence of oxaloacetate.

Citrate synthase activity was measured by placing 413 µl milliQ water, 50 µl DTNB (0.4mg.ml^{-1} in 1M Tris-HCl, pH 8.0, Boehringer Ingelheim), 2 µl Triton X-100 (10%), 5 µl mitochondrial preparation and 5 µl acetyl-CoA (6 mM) in disposable cuvettes. The rate increase (A1) was recorded at 412 nm on a BIO-TEK Uvikon UV-Vis double beam spectrophotometer for 2 min, followed by the addition of 25 µl oxaloacetate solution (1.32 mg.ml^{-1} in H_2O). The rate increase (A2) was followed for another 3 min. The activity was calculated using Equation 3.4.

Equation 3.4: Citrate synthase activity calculation

$$\text{CS activity} = [(A2-A1) / 13.6^{*}) \times 0.5 / (P \times (v/1000)] \times 1000$$
$$= \text{nmole.min}^{-1}.\text{mg}^{-1}$$

* Extinction coefficient for TNB = 13.6 mM^{-1}.cm^{-1}; V = volume (µl) mitochondrial preparation; P = protein concentration (mg.ml^{-1}).

3.5 Assessment of cell viability

This assay is based on cleavage of the tetrazolium salt 3-[4,5-dimethylthiazol-2-yl]-2,5-diphenyl-tetrazolium bromide (MTT) into a blue coloured product (formazan) by mitochondrial succinate dehydrogenase as seen in Figure 3.1. The conversion takes place only in living cells and the amount of formazan produced is proportional to the number of cells present (Denizot & Lang, 1986).

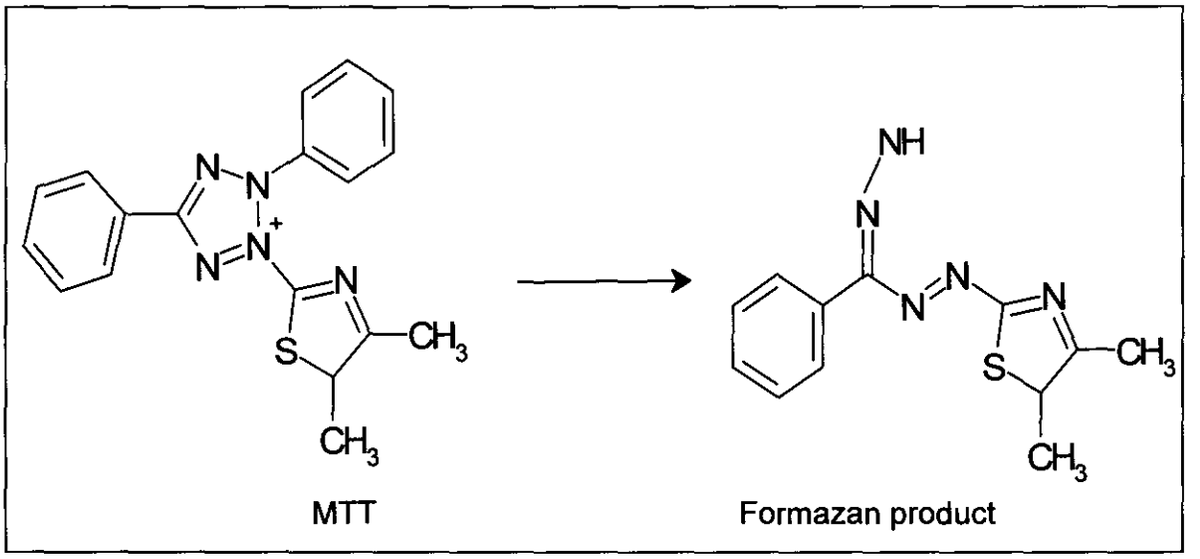

Figure 3.1: Molecular structure of MTT and the corresponding formazan product (adapted from Berridge, 1996).

HeLa cells were seeded in 96-well plates at a density 30 000, 20 000 and 15 000 cells per well for the 3, 24 and 48 hour incubations, respectively. The cells were left overnight to adhere to the bottom of the wells, after which the media was removed and 100 µl of freshly prepared media, containing the various concentrations of rotenone, *t*-BHP, $CdCl_2$ and $ZnCl_2$ (see Section 3.2.1) were added to the wells. Glacial acetic acid (final concentration 6%) was added as a positive control 30 min before each incubation time expired. After induction, the plate was centrifuge at 1000 x g for 5 min, and the media aspirated from each well. The plate was gently washed three times with 200 µl PBS, and centrifuged at 1000 x g for 5 min before 20 µl of MTT (Sigma-aldrich) (5 $mg.ml^{-1}$ in PBS) was added to each well. After a 5 hour incubation in a 5% CO_2 incubator, 100 µl of dimethyl sulphoxide (DMSO, Sigma-Aldrich) was added to each well, and the absorbance measured at 485nm (analytical) and 560nm (background) on a BIO-TEK FL600 fluorescence plate reader (Analytical & Diagnostic Products). The sample concentrations were normalised according to their protein content and expressed as percentage cell viability relative to the negative control group.

3.6 Reactive oxygen species assay

The intracellular ROS levels was detected by using 2',7'-dichlorofluorescein diacetate (H_2DCF-DA) (Sigma-Aldrich) probe. H_2DCF-DA is a cell-permeable indicator for ROS that is non-fluorescent until the acetate groups are removed by intra-cellular esterases and oxidation occurs within the cell. When oxidised by various reactive oxygen species, it is irreversibly converted to the fluorescent form 2',7'-dichlorofluorescein (DCF) (Wang & Joseph, 1999).

HeLa cells were seeded in a 96-well plate at a density of 30 000, 20 000 and 15 000 cells per well in a fixed volume of 100 µl, for the 3, 24 and 48 hour incubation respectively. The cells were left overnight to adhere to the bottom of the wells. The following morning, the media was removed and 100 µl of freshly prepared media, containing the various concentrations of rotenone, tBHP, $CdCl_2$ and $ZnCl_2$ were added to the wells as describe before (Section 3.2.1). After the induction period, 10 µl of H_2DCF-DA (Sigma-Aldrich) was added to each well (final concentration 10 µM) and incubated for 30 min at 37 °C. The plate was washed once with 200 µl PBS, before 100 µl of PBS was added to each well. Fluorescence was measured using a BIO-TEK FL600 fluorescence plate reader at 485 nm (excitation) and 530 nm (emmision) with an excitation setting (bias) set at 135. Sample concentrations were normalised according to their protein content and expressed as relative fluorescence units (RFU) per µg protein.

3.7 Confocal microscopy

HeLa cells were seeded on sterile coverslips in 6-well plates (NUNC) at a density of 200 000 cells per well in a fixed volume of 2 ml in culture medium. The cells were left overnight to adhere to the coverslips after which the media was removed and 2 ml of freshly prepared media was added that contained either EtOH (control) or rotenone at specific concentrations. Only the 100 nM and 2500 nM rotenone

concentrations were included in this analysis as well as the negative control (0 nM rotenone). These incubation were performed as described in Section 3.2.1.

After the 24 hour induction period, tetramethyrhodamine methyl ester (TMRM, Molecular Probes™[1]) at a final concentration of 0.5 μM and Mitotracker Green (Molecular Probes™) at a final concentration of 1 μM were added to the media and co-incubated for 30 min at 37°C. TMRM serve as a probe for membrane potential and Mitotracker Green as a specific probe for mitochondrial localisation. The coverslips of the cultured cells were washed with three changes of DMEM growth medium to remove any excess probes from the cytosolic compartment, before being mounted into a chamber. Confocal images were monitored using a Nikon (pcm2000) inverted confocal microscope. The images that were obtained used 505 nm (green) and 565 nm (red) excitation light from a krypton-argon-helium neon laser. Pinholes were set to about 0.5 μM with a neutral density filter of 10%.

3.8 Quantitative real-time Polymerase Chain Reaction (PCR)

3.8.1 Total RNA isolation

Harvested cells in PBS were centrifuged at 600 x g (5 min) before the supernatant was removed. The pellet was lysed by adding 500 μl of QIAzol™[2] Lysis Reagent (Qiagen, Hilden, Germany). Passing the lysate several times through the pipette tip completely disrupts the pellet. After a 5 min incubation period at room temperature, 100 μl of chloroform was added followed by vortexing for 15 seconds. The homogenised sample was incubated at room temperature for 5 min before centrifugation at 12 000 x g for 15 min at 4 °C. The upper phase was transferred to a sterile microcentrifuge tube before 250 μl of iso-propanol was added. The sample was incubated at room temperature for 10 min before centrifugation at 12 000 x g

[1] Molecular Probes is a trademark of Molecular Probes Inc., Eugene, OR, USA.

[2] QIAzol™ is a trademark of QIAGEN Pty Ltd., Hilden Germany.

for 10 min at 4 °C. The supernatant was removed and 500 µl of 70% EtOH was added to wash the RNA pellet, before the final centrifugation step at 7500 x g for 5 min at 4 °C. The supernatant was carefully discarded before the pellet was air dried and redissolved in 100 µl of RNase free water.

3.8.2 RNA concentration

The RNA concentration was determined using a BIO-TEK Uvikon UV-Vis double beam spectrophotometer (Analytical & Diagnostic Products) and calculated using the following equation:

Equation 3.5: RNA concentration

$$\text{RNA concentration} = [(A260nm - A320nm)/25] \times \text{dilution factor} = \mu g.\ \mu l^{-1}$$

The RNA integrity was electrophoretically verified by ethidium bromide staining and is discussed in Section 4.6.1.

3.8.3 cDNA Preparation

For the single strand synthesis of complementary DNA (cDNA) from total RNA samples, 1 µl of random hexamer primers (0.5 µg, Promega, USA) were added to 3 µg of isolated RNA in a PCR tube and incubated at 70°C for 5 min (step 1) to denaturate the RNA and ensure primer annealing. After the 5 min denaturation, the PCR tube was placed directly on ice. A reaction mix, composing of 1.25 µl dNTP (10 mM, Fermentas), 1 µl Moloney Murine Leukemia Virus Reverse Transcriptase (M-MLV RT, 200 units, Promega), 5 µl MLV buffer (Promega) and 11.75 µl of diethyl pyrocarbonate (DEPC) treated H_2O was added to the denatured sample. The cDNA synthesis was performed in a Thermo Hybaid Cycler (Bio-Rad) and the

conditions for the single strand preparation are described in Table 3.1. The single strand cDNA was stored at -20°C until use in real-time PCR.

Table 3.1: Conditions for preparation of single strand cDNA

Step	Number of cycles	Action	Temperature	Duration
2	1	Extension	37°C	60 min
3	1	Enzyme inactivation	80°C	10 min

3.8.4 Real-time PCR

This method involves detection of the binding of a fluorescent dye (SYBR Green) to double strand DNA (dsDNA). SYBR Green is a fluorogenic minor groove-binding dye that exhibits little fluorescence when in solution, but emits a strong fluorescent signal upon binding to the nascent double stranded DNA. When monitored in real-time, this results in an increase in the fluorescence signal that can be observed during the polymerization step and that diminishes when the DNA is denatured. Consequently, fluorescence measurements at the end of the elongation step of every PCR cycle are performed to monitor the increasing amount of amplified DNA (Bustin, 2000).

MT-IA, MT-IB, MT-IIA as well as 18S rRNA primers used for real-time PCR were designed using Primer 3 software (Rozen & Skaletsky, 2000). The primers were specified to be in different exons of the gene to prevent non-specific amplification due to genomic DNA (gDNA) and had to be less than 200 bp in length. Furthermore, primers had to contain approximately 50% G/C content. The primer sequences for Glyceraldehyde-3-phosphate dehydrogenase (GAPDH), β-actin, β-2-microglobulin and RNA polymerase II were obtained from Radonic *et al.* (2004). The primers used for the various genes investigated are summarised in Table 3.2.

Table 3.2: Primers used for Real-time PCR

Gene	Primers	Sequence	Amplicon size (bp)
MT-IA	MT-IA-Rev *	TTCCAAGTTTGTGCAGGTCA	185
MT-IB	MT-IB-Fwd MT-IB-Rev	GAACTCCAGGCTTGTCTTGG GATGAGCCTTTGCAGACACA	133
MT-IIA	MT-II-Fwd MT-II-Rev	TCCTGCAAATGCAAAGAGTG CAGGTTTGTGGAAGTCGCGT	187
GAPDH	GAPDH-Fwd GAPDH-Rev	GAAGGTGAAGGTCGGAGTC GAAGATGGTGATGGGATTTC	226
β-actin	Beta-Act-Fwd Beta-Act-Rev	AGCCTCGCCTTTGCCGA CTGGTGCCTGGGGCG	174
β-2-microglobulin	Beta-2-MG-Fwd Beta-2-MG-Rev	AGCGTACTCCAAAGATTCAGGTT ATGATGCTGCTTACATGTCTCGAT	306
RNA polymerase II	RP2-Fwd RP2-Rev	GCACCACGTCCAATGACAT GTGCGGCTGCTTCCATAA	267
18S rRNA	18S rRNA-Fwd 18S rRNA-Rev	GTGCATGGCCGTTCTTAGTT CGGACATCTAAGGGCATCAC	187

* MT-II-Fwd primer was used as Fwd primer with MT-IA-Rev primer for amplification. GAPDH, Glyceraldehyde-3-phosphate dehydrogenase; MT, Metallothionein; Fwd, forward primer; Rev, reverse primer.

A reaction mix, containing 10 µl iQ™ SYBR®[1] Green Supermix, 500 nM of forward and reverse primers (Inqaba Biotechnical Industries, RSA) and 75 ng of prepared cDNA (5 ng for 18S rRNA) in a final volume of 20 µl was subjected to the following PCR conditions listed in Table 3.3 for amplification in the iCycler iQ™[2] (Bio-Rad).

[1] iQ™ SYBR®[1] is a registered trademark of Molecular Probes Inc., Eugene, USA.

[2] iCycler iQ™ is a trademark of Bio-Rad, Hercules, Canada.

Table 3.3: PCR conditions for amplification

PCR step	Number of cycles	Action	Temperature	Duration
1	1	Denaturation	95 °C	3 min
2	30	Denaturation	95 °C	20 s
		Primer Annealing	60 °C	10 s
		Extension	72 °C	20 s
		Fluorescence measurement	82 °C[b]	5 s
3	1	Extension	72 °C	5 min
		Denaturation	95 °C	1 min
4	1	Annealing	55 °C	1 min
5	80	Melting curve program[a]	55-95 °C	5 s

[a] Heating rate of 0.5 °C per 5 seconds and fluorescence measurement every 5 seconds.
[b] 84 °C for 18S rRNA.

A high temperature fluorescence measurement point at the end of the fourth step was performed to improve SYBR Green quantification (Pfaffl *et al.*, 2002). Fluorescence was measured following each cycle and displayed graphically (iCycler iQ Real-time Detection System Software, version 3.0). The software determines a cycle threshold (Ct) value, which was defined as the number of PCR cycles where fluorescence signal exceeds the detection threshold value for that sample. This threshold is set to the exponential range of the amplification curve and kept constant for data analysis throughout the study. Every assay included a no-template control, five serial dilution points (in steps of 5 folds) of a cDNA mixture, as well as each of the test cDNA's. All samples were amplified in triplicate and the mean value was used for further calculations.

PCR efficiency for each primer set was calculated by the comparative Ct method using the REST software tool (Pfaffl *et al.*, 2002) and gene expression stability for

housekeeping genes was analysed using the GeNorm software tool (Vandesompele *et al.*, 2002).

3.9 Competitive Enzyme-Linked Immunosorbent Assay (ELISA)

3.9.1 Sample preparation

Cells were harvested as described in Section 3.2.2, and centrifuged at 600 x g for 5 min before the supernatant was removed. The pellet was redissolved in 500 µl of 1% Tween 20®[1] (Polyoxyethylensorbitonmonolaurat, Merck) in PBS, before a 20 second sonication. The sonicated sample was centrifuged at 12 000 x g for 5 min and the supernatant transferred to a new microcentrifuge tube. The samples were stored at –70°C until use in assay.

3.9.2 Method

Enzyme immunoassays combine the specificity of antibodies with the sensitivity of simple spectrophotometric enzyme assays by using antibodies or antigens coupled to an easily assayed enzyme that also possesses a high turnover number. In a competitive ELISA, the sample and antibody is co-incubated overnight before it is added to the capture antigen. The amount of colour development is inversely proportional to the amount of antigen present in the sample (Wilson & Walker, 1994).

The ELISA assay was performed in principle as described by Buther *et al.* (2002) with major modifications that was subsequently included. Known concentrations of MT from rabbit liver (Sigma-aldrich) were prepared in microcentrifuge tubes as

[1] Tween 20® is a registered trademark of ICI Americas Inc., Wilmington, DE, USA.

follows: 200, 100, 50, 25, 12.5, 6.25, 3.125, 1.533, 0.781, 0.391, 0.195, and 0 $\mu g.\mu l^{-1}$, respectively, in a total volume of 160 µl. These cellular standards were incubated overnight at 4°C with 160 µl of rabbit polyclonal antibody (Biogenesis, England), dilution 1:1000 in 1% Tween 20® in PBS. The cellular samples were thawed and diluted to a final protein content of 250 $\mu g.160\ \mu l^{-1}$ and incubated with 160 µl primary antibody overnight. The wells of a 96-well Nunc-Immunoplate (Maxisorb surface, Nunc) were coated with 100 µl of 4 $\mu g.ml^{-1}$ MT from rabbit liver, diluted in 0.1 M $NaHCO_3$ (pH 9.6). The plate was incubated overnight at 4 °C, to allow the MT to adhere to the maxisorp plate.

Subsequent to the overnight incubation, the plate was decanted and washed three times with 200 µl washing buffer (0.05% Tween 20® in PBS) for 5 minutes on an orbital shaker at room temperature, before 200 µl blocking buffer (0.3% bovine serum albumin (BSA), 0.05% Tween 20® in PBS) was added. The plate was incubated for 2 hr on an orbital shaker at room temperature. After this blocking step, the plate was again washed three times with washing buffer, before 100 µl of each standard and sample was added to the plate in triplicate and incubated for a further 60 min. The plate was subsequently washed five times with washing buffer, before 100 µl goat anti rabbit IgG: HRP-conjugated (Zymed®[1]), at a dilution of 1:5000 in blocking buffer, was added and incubated for another 60 min. Washing of the plate was performed as previously described, after which 100 µl of a 3,5,3',5'-tetramethylbenzidine (TMB) (Zymed®) solution was added. As soon as a blue colour developed, the reaction was stopped with 1 M HCl after which a yellowish colour appeared. The absorbance was measured at 460 nm on a BIO-TEK FL600 fluorescence plate reader (Analytical & Diagnostic Products). Sample MT concentrations were calculated using a MT standard curve (semi-logarithmic scale) and expressed as an X fold increase relative to the control group.

[1] Zymed® is a registered trademark of Zymed laboratory Inc., San Francisco, CA, USA.

3.10 Protein content assay

The bicinchoninic acid (BCA) method was used in this study to determine protein content of samples and cells. This method, which in principle is similar to the Lowry method relies on the formation of a protein complex between divalent copper ions and peptide bonds under alkaline conditions, where the copper becomes reduced to monovalent ions. These monovalent ions react with BCA to produce an unstable product that becomes reduced to molybdenum/tungsten blue. The advantage of BCA is that the reagent is fairly stable under alkaline conditions and can be included in the copper solution to allow a one step procedure (Stoscheck, 1990).

In the standard assay 10 µl of sample or standards was mixed with 200 µl of a solution of BCA: $CuSO_4.5H_2O$ (50:1) in a 96-well microtiter plate. The samples were incubated for 20 min at 37°C and the absorbance measured using a BIO-TEK FL600 fluorescence plate reader at 560 nm. The amount of protein in the samples was quantified using a standard curve prepared from a standard series containing BSA (Sigma-aldrich).

3.11 Presentation of results and statistical analysis

The results of this study are presented both in tabular and graphical form. The tables contain the mean and experimental parameters measured, as well as the standard deviation (stdev) for each of the rotenone, $CdCl_2$, $ZnCl_2$ and *t*-BHP treated groups. Statistical analyses were performed on all of the data using Statistica©[1] Version 6.1 software.

The basic Student T-test is the most commonly used statistical method to evaluate the differences in means between two group, as long as the variables are normally

[1] Statistica© is a copyright of StatSoft, Tulsa, OK, USA.

distributed within each group and the variation of data in the two groups is not different. If the variables are not normally distributed, then the differences in means between the two groups can be evaluated using one of the nonparametric alternatives to the T-test.

Mean values of rotenone treated groups that are statistically significantly different from that of the control group ($p<0.05$) using the Student T-test are indicated with an asterisk. Graphs were compiled using Microsoft®[1] Excel software and include stdev bars.

[1] Microsoft®[1] is a registered trademark of Microsoft Corporation, Redmond, WA, USA.

CHAPTER FOUR

RESULTS AND DISCUSSION

4.1 Introduction

This Chapter contains the results and discussion of the experimental methods as described in Chapter Three, as well as clarification on some of the experimental approaches. The statistical methods used in the analysis of the data were described in Section 3.11.

4.2 OXPHOS analyses

4.2.1 NADH:ubiquinone oxidoreductase

The activity of NADH:ubiquinone oxidoreductase was expressed as a percentage of the mean of control values relative to the mitochondrial matrix enzyme and is listed in Table 4.1. The results indicated that with rotenone incubation from 0 to 2500 nM, an initial decrease in complex I activity could be observed before a surprising sharp increase in activity with 1000 nM incubation. No complex I activity could be detected at 2500 nM. Due to the obvious variability in the assay, none of the values obtained for any of the incubations were significantly different from the control group.

This problem with variability of this particular assay was ob served in a number of similar experiments and it became clear that the particular assay for measuring the enzyme was not accurate enough, i.e. rotenone-sensitive activity could not accurately be measured. It was decided to utilise a different approach to measure the activity of complex I, that is through the measurement of a combined complex I and III activity.

Table 4.1: NADH:ubiquinone activity of different rotenone concentrations

Rotenone (nM)	% Activity	Mean ± stdev*	*p*
0	100.0	478±198	-
10	71.4	341±286	0.53
100	60.1	287±384	0.49
1000	234.3	1120±982	0.33
2500	0.0	0±691	0.06

*Activities are expressed as nmoles per min per unit citrate synthase (n = 3).

4.2.2 Combined complex I + III assay and complex III

The activity of the combined complex I + III is expressed as a percentage of the control group as summarised in Table 4.2, with the result for complex III listed in Table 4.3. Figure 4.1 illustrates both the activities measured in the same series of mitochondrial preparations of rotenone treated (24 hour) HeLa cells. A decrease in the combined complex I+III activity (blue) is observed in Figure 4.1 from 100 - 0% with an increase in rotenone concentration. The activity decreased by 50% with 10 nM rotenone and is completely absent at 2500 nM rotenone. The activity in complex III (purple) remained approximately the same for each of the rotenone concentrations, indicating that the decrease in the combined complex I+III activity were as a result of a deficiency in complex I only. These results indicated that complex I deficient HeLa cells with different degrees of deficiency could be induced, thus establishing an *in vitro* model for complex I deficiency where the expression of metallothionein (MT) and selected biochemical parameters could be investigated.

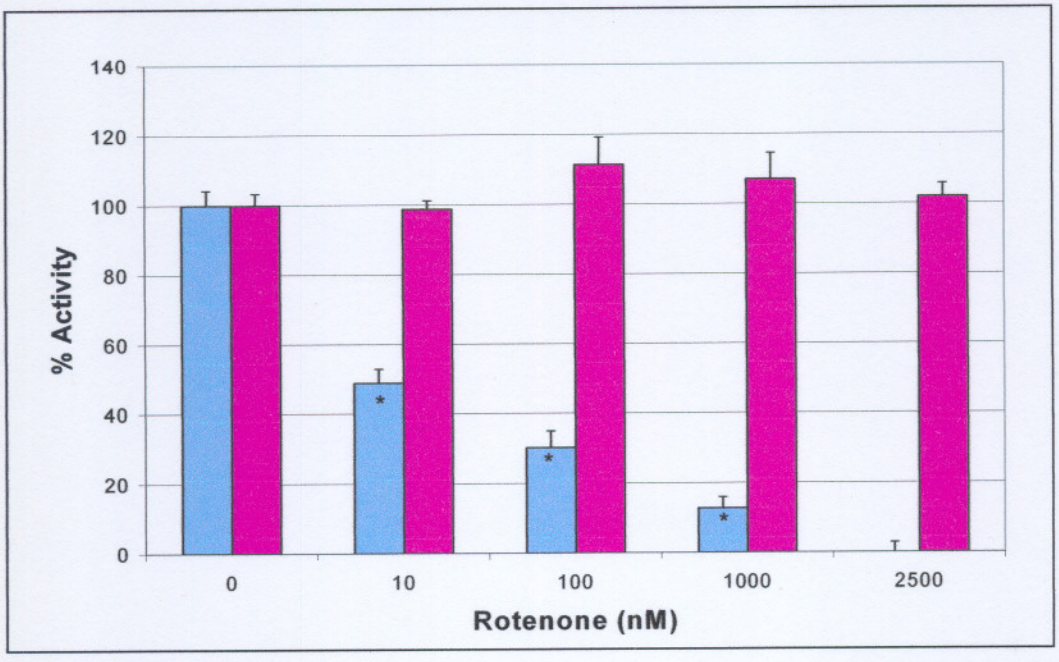

Figure 4.1: Complex I+III (rotenone sensitive) activities and complex III activities in HeLa cells incubated with rotenone. Values (Table 4.2 and 4.3) are expressed as percentage of control (0 nM) ± stdev (n = 2). Asterisk indicates mean values that are statistical significant using the Student T-test to the control group. Complex I+III (blue) and complex III (purple) are indicated separately at different rotenone concentrations.

Table 4.2: Combined complex I and III activity

Rotenone Concentration	% Activity	Mean ± stdev *	*p*
0	100.0	124.9±4.3	-
10	48.8	60.9±4.1	0.88
100	30.2	37.8±4.7	0.36
1000	12.7	15.9±3.2	0.50
2500	0.0	0.0±2.8	0.80

*Activities are expressed as nmoles per min per unit citrate synthase. (n = 2).

Table 4.3: Complex III activity

Rotenone Concentration	% Activity	Mean ± stdev *	*p*
0	100.0	61.5±3.3	-
10	98.8	60.8±2.5	0.00
100	111.3	68.5±7.9	0.00
1000	107.0	68.9±7.5	0.00
2500	101.9	62.7±3.8	0.00

*Activities are expressed as nmoles per min per unit citrate synthase. (n = 2).

4.3 Assessment of cell viability

4.3.1 Optimisation of method

For the viability (MTT) assay, the seeding density of HeLa cells for the 3, 24 and 48 hour incubation periods were chosen to avoid a 100% confluency of the positive and negative control wells. During the optimisation of the method different conditions were utilised with regard to the positive control. The positive control for the assessment of cell viability must be a reagent that is known to be toxic to cells. Initially, Triton X-100 (final concentration of 0.1%) was used, but it caused detachment of the cells from the bottom of the plate resulted in the loss of cells during the washing steps. Different concentrations of *t*-BHP (10 and 50 mM) were subsequently used, and as indicated in Figure 4.2, the incubation time of 30 minutes was not sufficient to cause any damage to the cell membranes of the cells. Another condition that was utilised was different acetic acid concentrations (0.5, 1, 3, and 6%). In Figure 4.2, the different positive controls are indicated together with their respective standard deviations as percentage cell viability with regard to the negative control.

The results shown in Figure 4.2 indicate that 6% acetic acid, with a cell viability of only 3.4%, had the lowest viability that could be accurately measured. This was subsequently used as the positive control in the assay. It should be noted that cell

viability also is dependent on the number of cells that are attached to the bottom of each well. The lower the number of cells, the lower the cell viability appears to be as seen in the case with Triton X-100. Cells was quantified by determining the protein content after the intervention as described in section 3.10.

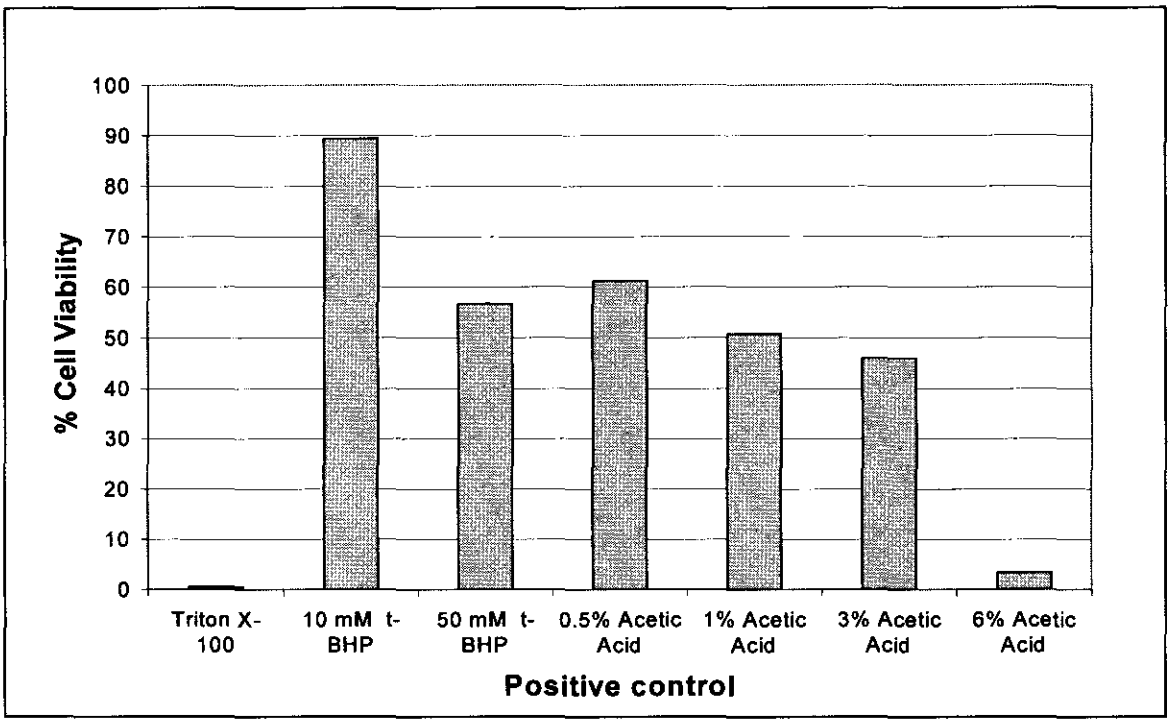

Figure 4.2: Positive controls utilised for cell viability assessment (MTT test). The graph shows the different positive controls used for the MTT test as discussed in Section 4.3.1. Results are expressed as percentage cell viability where the negative control (untreated HeLa cells) is 100%.

4.3.2 Effect of rotenone on cell viability

The cell viability (MTT test) was expressed as a percentage of the median values relative to the control group, and the results are listed in Table 4.4 and illustrated in Figure 4.3. The asterisk indicates the concentrations that are significantly different from that of the control group of each induction period. The three hour incubation period (blue) illustrates an initial decrease in cell viability with an increase in

rotenone concentration as displayed in Figure 4.3. A slight increase in cell viability is observed at the 100 nM rotenone concentration with a viability of 106%. Another decrease at 1000 nM is observed relative to the 100 nM concentration, with an increase in the cell viability at the 2500 nM rotenone induction. The positive controls ($CdCl_2$ and $ZnCl_2$) illustrate a slight decrease compared to the negative control, at 3 hours and 24 hours.

The 24 hour induction period (red column) also showed a slight increase in cell viability with the 0 and 100 nM rotenone concentrations, before a decrease is observed with the remaining concentrations. The results that were obtained for the 48 hour period (yellow column) illustrated the same general trend that was seen with the three hour induction period. Although this method is mainly sensitive to cellular necrosis, it must be kept in mind that under non-ideal cell culture conditions, for example a decrease in pH, the results may vary greatly (Berridge, 1996; Plumb *et al.*, 1989). The effect of the pH has been visually observed with the colour of the media (which contains phenol red) changing from red to orange-yellow. The more orange the media became, as has occurred with the 48 hour incubation series, the lower the pH became and may have affected those results independent from the contribution of rotenone. The media could not be changed at any time during the incubation periods. The reasons for this is, firstly, that if the incubation media were replaced again with rotenone-containing media the effective cellular rotenone content will be increased as rotenone binds irreversibly to complex I and, secondly, if the media were replaced with media not containing rotenone the "fresh" media will allow the cells to recover to a certain extent.

In conclusion, however, the results did indicate that cell viability, or more accurately the cell's ability to metabolize MTT to form formazan, decreased with a decrease in complex I deficiency. In light of the severe decrease in complex I activity the decrease in viability, or increase of necrosis, was surprising slow.

Table 4.4: Data obtained from cell viability (MTT test) in HeLa cells using rotenone

Time (hr)	Rotenone (nM)	% Cell viability	Mean ± stdev *	*p*
3	PC**	4.0	0.01±0.00	0.00
	NC**	100.0	0.30±0.01	0.00
	0	95.3	0.26±0.01	-
	10	86.7	0.26±0.01	0.70
	100	106.1	0.28±0.01	0.03
	1000	92.5	0.28±0.01	0.01
	2500	95.2	0.29±0.02	0.01
	$CdCl_2$***	81.0	0.30±0.01	0.00
	$ZnCl_2$***	97.2	0.28±0.03	0.10
24	PC**	3.6	0.01±0.00	0.00
	NC**	100.0	0.24±0.03	0.01
	0	110.1	0.35±0.06	-
	10	120.6	0.37±0.02	0.39
	100	68.1	0.35±0.01	0.95
	1000	66.2	0.26±0.03	0.02
	2500	52.7	0.22±0.01	0.00
	$CdCl_2$***	74.1	0.30±0.02	0.12
	$ZnCl_2$***	78.7	0.35±0.01	0.91
48	PC**	2.8	0.01±0.00	0.00
	NC**	100.0	0.65±0.04	0.45
	0	141.4	0.62±0.02	-
	10	115.8	0.73±0.05	0.01
	100	125.9	0.70±0.05	0.04
	1000	89.6	0.33±0.01	0.00
	2500	70.4	0.23±0.01	0.00
	$CdCl_2$***	102.9	0.45±0.01	0.00
	$ZnCl_2$***	112.0	0.70±0.02	0.01

*Mean values are expressed as absorbance. (n = 2);** PC = 6% acetic acid; **NC = negative control (untreated HeLa cells).***$CdCl_2$ (12.5 µM) and $ZnCl_2$ (250 µM) used as positive controls for metallothionein expression.

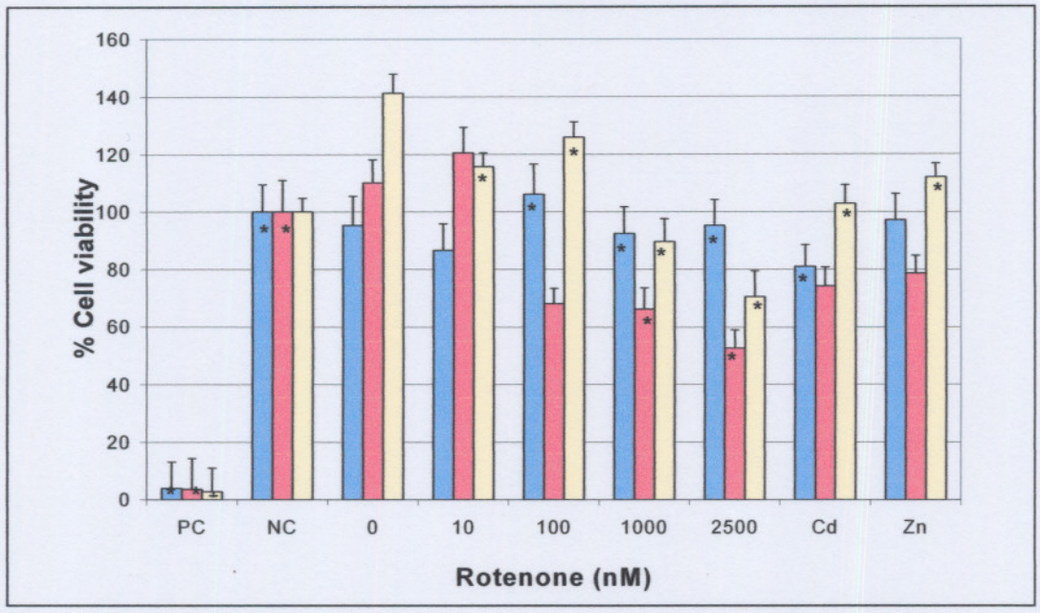

Figure 4.3: Effect of rotenone on cell viability (MTT test) in HeLa cells. The percentage viability of HeLa cells treated with rotenone was measured with the MTT test. Results are expressed relative to the negative control cells (NC) which had no addition of rotenone or ethanol ± stdev (n = 5). The positive control (PC) were 6% acetic acid (Figure 4.2) and Zn and Cd where also included as controls. Viability was measured in separate experiments over 3 (blue), 24 (red) and 48 (yellow) hours. The asterisk indicates mean values that are statistically significantly different from the control group using the Student T-test. Note that the 100 nM (3 hour) is indeed significantly different from the control group.

4.3.3 Effect of *t*-BHP on cell viability

The cell viability results obtained with different *t*-BHP concentrations are graphically illustrated in Figure 4.4. The asterisk indicates the concentrations that are significantly different from the control group which were HeLa cells cultured under normal conditions. The viabilities of *t*-BHP treated cells were significantly different from the control group and ranged from 40 - 44% as illustrated in Figure 4.4. The mean value for the 0.5-, 0.8- and 1 mM concentrations of *t*-BHP was 0.12 ± 0.01, 0.11 ± 0.01 and 0.11 ± 0.01 respectively. As mentioned in Section 4.3.2, the pH of the culture media plays a critical role in the significance of results that are obtained. The incubation medium with *t*-BHP also had a visible, although slight, change in pH. The amount of cells that remained in the wells after the induction period compared

to the control were notably different and, as mentioned in Section 4.1.1, although the result is normalised to the amount of protein in the well, the assay is optimised to a certain amount of cells present in each well. Nevertheless, these results indicate that the MTT assay will indicate a dose-dependent loss in cellular viability with an increase in oxidative stress induced by *t*-BHP. This supports the data obtained from the rotenone incubations where oxidative stress-related damage is putatively also occurring and probably the main reasons for loss in cell viability.

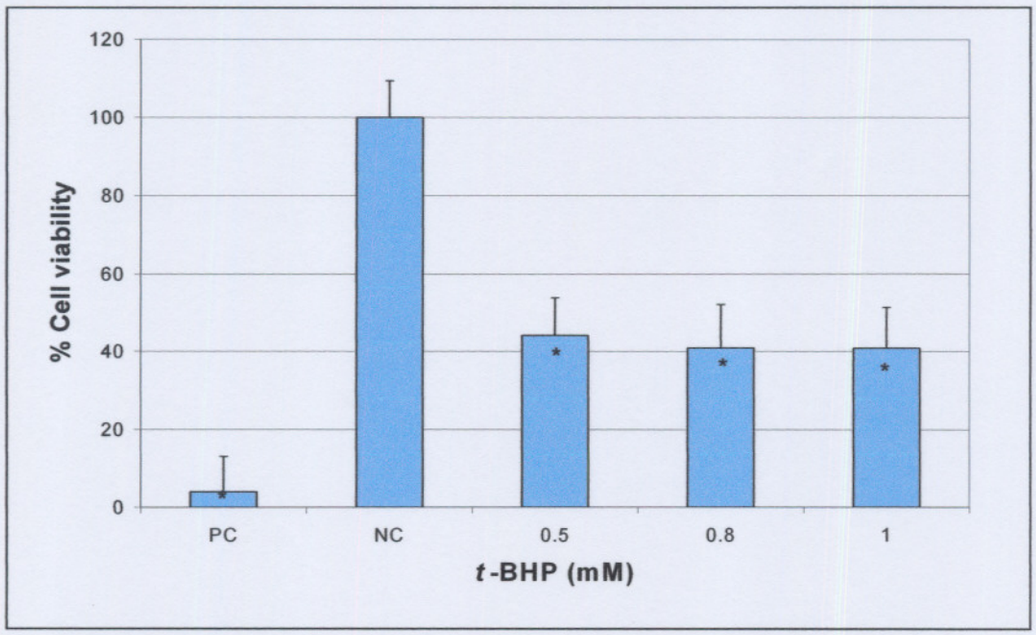

Figure 4.4: Effect of *t*-BHP on cell viability (MTT test). Values indicate percentage viability ± stdev of HeLa cells incubated for 3 hour with different concentrations of *t*-BHP relative to the negative control (NC) which were untreated. The positive control (PC) was 6% acetic acid. The asterisk indicates mean values that are statistically significant to the control group using the Student T-test.

4.4 Reactive oxygen species assay

4.4.1 Optimisation of method

The seeding density for this assay was once again chosen to avoid 100% confluency of the positive and negative controls as discussed in Section 4.2.1. Cells were initially seeded (15 000 and 30 000 cells per well) for a three hour induction period in a trial run of the method. The probe, H_2DCF-DA, was diluted in the culture media or PBS to a final concentration of 10 μM. From this trial run (data not shown), it was found that the probe are more stable when dissolved in culture media and the reproducibility were better than when dissolved in PBS. The protein content, which represents the amount of cells present in the wells, was measured and used to normalise the result (measured in relative fluorescence units).

4.4.2 ROS production measurement in rotenone-treated HeLa cells

In this assay the negative control that was used were cells that had no rotenone and each rotenone concentration as well as the positive controls was compared to this negative control. The data is summarised in Table 4.5 and graphically illustrated in Figure 4.5. An increase from 0 to 7764 RFU per μg protein is observed indicating a significant increase in ROS production as the rotenone concentration increase. Furthermore, the amount of ROS produced with a rotenone concentration of 2500 nM increased from 198 to 7764 RFU per μg protein between the 3 hour and 48 hour incubation periods.

As indicated in Section 4.6.3.2, $CdCl_2$ significantly induces MT expression which can scavenge ROS and explain the lower levels detected in the control. Furthermore, to explain the lower ROS levels at 10 nM rotenone, production of antioxidant enzymes, such as SOD, initially take place when oxidative stress occurs. These antioxidant enzymes can initially lower ROS levels up to a certain extent, before the capacity is overwhelmed, such as might occur at higher rotenone levels.

Table 4.5: Rotenone induced ROS production at different incubation times

Time (hr)	Concentration	RFU. μg^{-1} protein	Mean ± stdev *	*p*
3	0	0.0	2167±11.7	-
	10	133	2312±14.7	0.02
	100	-137	2082±11.5	0.32
	1000	-23	2233±5.4	0.31
	2500	198	2375±5.1	0.00
	$CdCl_2$**	365	2479±14.6	0.00
	$ZnCl_2$**	787	3044±12.1	0.00
24	0	0.0	1840±125.4	-
	10	-26	1833±180.7	0.93
	100	340	2204±171.8	0.00
	1000	1523	3342±322.6	0.00
	2500	1609	3534±242.9	0.00
	$CdCl_2$**	-219	1596±127.3	0.00
	$ZnCl_2$**	631	2439±199.3	0.00
48	0	0.0	1651±296.7	-
	10	-443	1317±345.5	0.08
	100	2178	3930±291.6	0.00
	1000	1929	3646±234.7	0.00
	2500	7764	9578±263.9	0.00
	$CdCl_2$**	-86	1587±326.1	0.71
	$ZnCl_2$**	354	2288±642.0	0.03

*ROS production is expressed as RFU per μg protein. (n = 7);** $CdCl_2$ (12.5 μM) and $ZnCl_2$ (250 μM) used as positive controls for metallothionein expression.

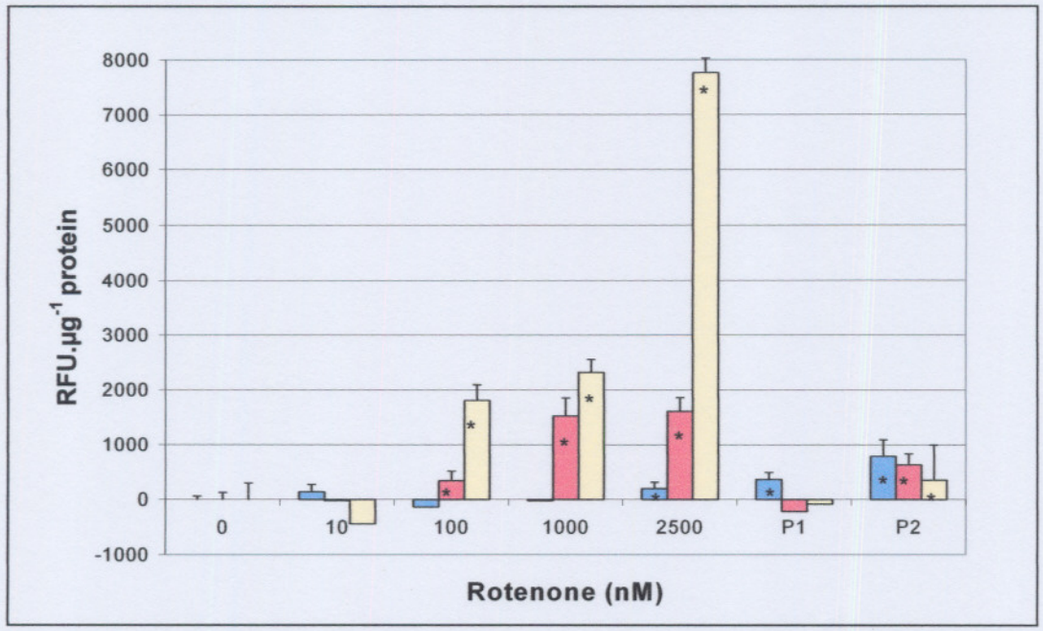

Figure 4.5: ROS production in HeLa cells treated with rotenone. Results are expressed as relative fluorescence units per µg protein ± stdev (n = 7). The production of ROS in HeLa cells, treated with different concentrations of rotenone as well as $CdCl_2$ (P1, 12.5 µM) and $ZnCl_2$ (P2, 250 µM) is shown (y-axis). The incubations where performed in separate experiments over 3 (blue), 24 (red) and 48 (yellow) hours. The asterisk indicates mean values that are statistically significant to the control group (0 nM).

4.4.3 ROS production of HeLa cells treated with *t*-BHP

The negative control utilised in this assay was normal HeLa cells cultured under the same conditions as the experimental group. The value of the negative control was subtracted from the different concentrations of *t*-BHP to obtain relative quantification for each concentration and is graphically illustrated in Figure 4.6. The induction by *t*-BHP from 0.5 mM (3388 ± 542.3 RFU per µg protein) to 1 mM (4873 ± 3152.2 RFU per µg protein) shows an increase in ROS production with an increase in t-BHP concentration. The stdev of 1 mM is quite high, indicating high variability between the replicates. These results correlate not only with what we were expecting, but also with the results from Heo *et al.* (1997) where increased lipid peroxidation was observed in a dose-dependent manner using *t*-BHP as ROS producer.

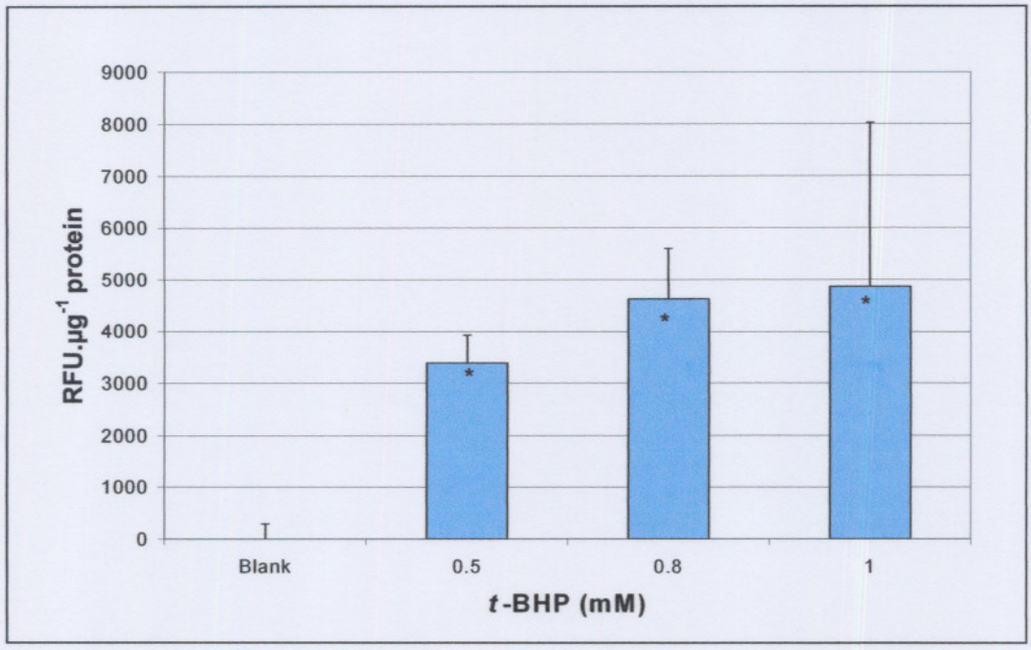

Figure 4.6: ROS production with different *t*-BHP concentrations. Results are expressed relative to the untreated control group ± stdev (n = 7). The production of ROS in *t*-BHP treated HeLa cells is expressed as relative fluorescence units per µg protein. The asterisk indicates mean values that are statistically significant to the control group using the Student T-test.

4.5 Confocal microscopy

4.5.1 Membrane potential assessment of HeLa cells

TMRM is a membrane permeable cationic fluorophore that loads into polarised mitochondria due to the negative membrane potential of the mitochondria. When excited with green light, TMRM-labeled mitochondria appears as spots of bright red fluorescence as indicated in Figure 4.7. With a loss in membrane potential (depolarisation), TMRM ceases to identify the mitochondria which become invisible (Elmore *et al.*, 2004).

Figure 4.7 illustrates the membrane potential of HeLa cells treated with different concentrations of rotenone for 24 hours. A decrease in membrane potential is

observed between the control and the rotenone treated groups. This suggests that with increased rotenone concentration, a decrease in membrane potential occurs. This may be due to increased ROS-related damage or opening of the mtPTP, which is known to occur at excessive oxidative stress and which is also an apoptosis-related occurrence. The experimental setup was not ideal to view the decrease in membrane potential of the same cell as can be achieved with confocal microscopy due to the long incubation time with a consequent quenching of the fluorescence of the probes.

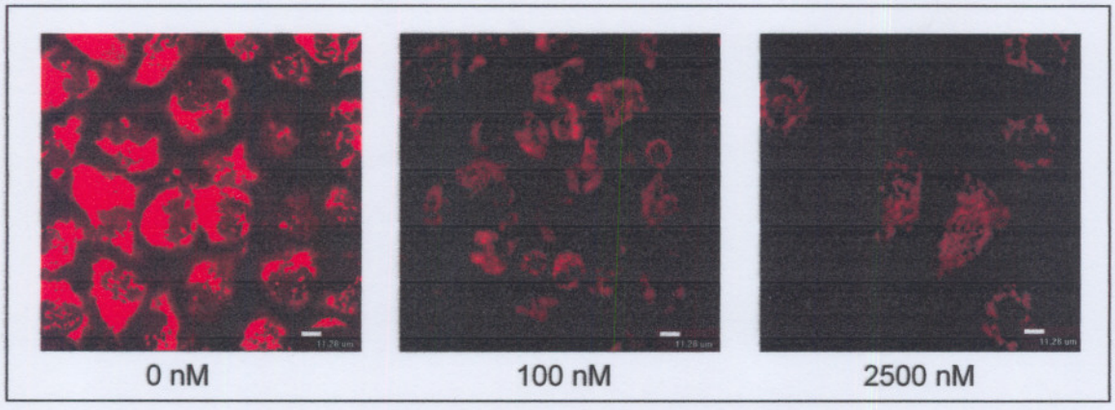

Figure 4.7: Rotenone treated HeLa cells stained with TMRM and Mitotracker green. The red fluorescence indicates TMRM stained mitochondria of the control group (0 nM), as well as different rotenone concentrations (100 nM and 2500 nM), incubated for 24 hours.

4.6 Quantitative real-time Polymerase Chain Reaction (PCR)

4.6.1 RNA concentration

The RNA concentrations of rotenone treated HeLa cells for the various incubations periods ranged between 0.02 and 4.12 $\mu g.\mu l^{-1}$, with an A260/A280 ratio of between 1.3 and 1.9. The A260/A280 ratio provides an estimate of the RNA purity of each sample with respect to contaminants that absorb in the ultraviolet (UV) region, such as protein and phenol. A ratio of 1.9 - 2.1 in 10 mM Tris-Cl (pH 7.5) is an indication

of high purity. The ratio is influenced considerably by pH, and since water is not buffered, the pH and the resulting A260/A280 ratio can vary greatly. As described in Section 3.8.1, the isolated RNA sample was dissolved in water, and can thus explain the variation in the ratios of the samples.

For the 48 hour induction period, the flasks were seeded at approximately 60% confluence to prevent the cells from becoming confluent too fast and subsequently stressed. This precaution unfortunately also resulted in very low RNA yields for the highest concentration (2500 nM). This incubation was repeated with a flask that was approximately 70-80% confluent but still resulted in a RNA yield of 0.02 $\mu g.\mu l^{-1}$ that was not sufficient to use for cDNA preparation.

4.6.2 Integrity of RNA samples

Intact total RNA that are run on a 1% agarose gel will have sharp, clear 28S and 18S rRNA fragments similar to those displayed in Figure 4.8, lane C. The 28S rRNA band should be approximately twice as intense as the 18S rRNA band. This 2:1 ratio (28S:18S) is a good indication that the RNA is intact as observed in Figure 4.8. Partially degraded RNA will have a smeared appearance, and either lacks the sharp rRNA bands or does not exhibit the 2:1 ratio of the rRNA. Completely degraded RNA (Figure 4.8, lane B) will appear as a very low molecular weight smear (Wilson & Walker, 1994). RNA samples isolated in this study were all checked for quality on a 1% agarose gel and only those samples that were found to be of good quality were used in cDNA synthesis.

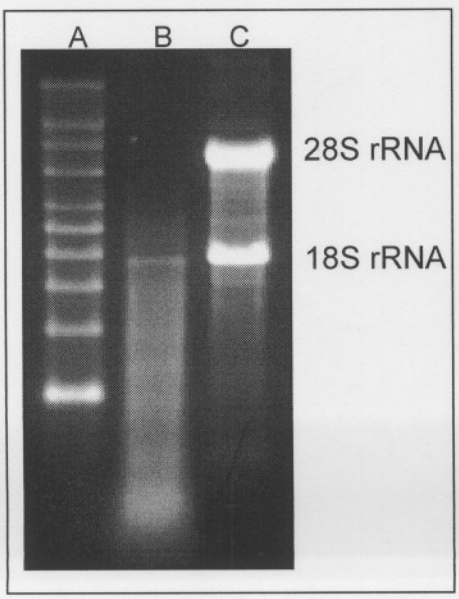

Figure 4.8: Intact RNA vs degraded RNA. Two micrograms of degraded and intact total RNA was run on a 1% agarose gel with a RNA marker (A). The 18S and 28S rRNA fragments are clearly visible in the intact RNA sample (C). The degraded RNA appears as a low molecular weight smear (B).

4.6.3 Real-time PCR

4.6.3.1 Optimisation of method

MT-IIA and MT-IB primers were initially used in this study but very low levels (baseline levels) of MT-IB expression were detected in cDNA prepared from any of the HeLa cell preparations. The more common form of the MT-I isoforms, MT-IA was also investigated, but no expression was detected either. The primer functionality was validated in PCR amplification with gDNA as template and specific products were distinguished, thus ruling out any problems with regard to the primers or PCR efficiency.

The data that are presented in Section 4.6.3.2 were normalised using housekeeping genes as controls to account for sample handling, loading and experimental variation. The suitability of different housekeeping genes (as seen in Table 3.2) were investigated by Levanets *et al.* (See Appendix A). As discussed in Appendix A, the rank of these housekeeping genes' expression stability in conditions of rotenone induced HeLa cells was 18S rRNA, β-2-microglobulin, GAPDH, β-actin and RNA polymerase II. The transcription variation of the housekeeping genes were not more than two, thus making all of these genes suitable as internal controls.

4.6.3.2 Metallothionein RNA expression in HeLa cells induced with rotenone and *t*-BHP

Quantitative real-time PCR was performed on RNA samples of HeLa cells treated with different concentrations of rotenone or *t*-BHP using MT-IIA primers (Table 3.2) and normalised with the three most stabile housekeeping genes (18S rRNA, β-2-microglobulin and GAPDH). Results are listed in Table 4.8 (rotenone) and Table 4.9 (*t*-BHP) as fold change expression ratios relative to the control group (0 nM) and are graphically illustrated in Figure 4.9 and Figure 4.10 for rotenone and *t*-BHP treated cells, respectively. Three additional rotenone concentrations; 1, 5 000 and 10 000 nM were included in the 24 hour induction period. The fold

change expression ratio of all the samples ranged between 1 and 7, except for $CdCl_2$ that have an expression ratio of 48.9. The y-axis scale was fixed between 0 and 10 units for optimal illustration of the difference in expression between the rotenone concentrations.

A general increase in MT expression is observed with an increase in rotenone concentration as well as between the different induction periods. $CdCl_2$ showed the highest metallothionein induction with a fold change of approximately 49 whereas surprisingly, $ZnCl_2$ treatment did not induce MT-IIA expression as baseline levels were obtained. A rstudy by Yurkow and DeCoste (1999) also showed that zinc does not markedly increase MT in lymphocytes compared to the dramatic induction with cadmium. The variation of MT expression over a three hour induction period could be as a result of the incubation time that was too short to induce MT expression. The 2500 nM induced rotenone concentration over 24 hours showed the highest MT expression with regard to rotenone. It is not known whether 2500 nM during 48 hours would has shown an increase in expression as it have been excluded from this investigation due to low RNA yields (Section 4.6.2). The increased MT expression of 100 nM in relation to 1000 nM was not expected and may suggest a critical point for MT induction or ROS release from mitochondria that needs to be investigated further.

Figure 4.10 illustrates the fold change expression ratios of *t*-BHP induction relative to the control group (0 nM rotenone). An increase in expression from 2 (0.5 mM) to 5 (1 mM) is observed during 3 hrs of induction with *t*-BHP. This result correlates with the increase in ROS production that was illustrated by Figure 4.6. Although rotenone did not induce MT during the same induction period, it should be taken into consideration that *t*-BHP is a direct inducer of ROS, whereas rotenone induces a deficiency of complex I that results in ROS production. This data suggest that MT is not only induced by metals ($CdCl_2$) but may also be induced by ROS.

Table 4.8: Expression ratios of HeLa cells induced with rotenone

Time (hr)	Rotenone (nM)	Expression ratio*	*p*
3	**0**	1.0±0.11	-
	10	1.4±0.22	0.03
	100	0.8±0.12	0.00
	1000	0.9±0.11	0.05
	2500	1.2±0.08	0.00
24	**0**	1.0±0.09	-
	1	1.1±0.25	0.28
	10	1.2±0.18	0.07
	100	3.0±0.80	0.00
	1000	2.3±0.27	0.01
	2500	6.8±1.66	0.00
	5000	6.6±1.02	0.00
	10 000	6.6±0.82	0.00
	$CdCl_2$* **	48.9±5.49	0.00
	$ZnCl_2$* **	1.0±0.12	0.15
48	**0**	1.0±0.14	-
	10	1.5±0.19	1.00
	100	3.5±0.27	0.00
	1000	2.7±0.19	0.02

*Expression ratio is normalized against 18S rRNA, β-2-microglobulin and GAPDH and is expressed as fold change with stdev. (n = 3). ***$CdCl_2$ (12.5 µM) and $ZnCl_2$ (250 µM) where included as positive controls for metallothionein expression.

Table 4.9: Expression ratios of HeLa cells induced with *t*-BHP

Time (hr)	*t*-BHP (mM)	Expression ratio*	*p*
3	**0**	1.0±0.19	-
	0.5	2.0±0.17	0.00
	0.8	4.6±1.09	0.00
	1	5.1±0.66	0.050

*Expression ratio is normalized against 18S rRNA, β-2-microglobulin and GAPDH and is expressed as fold change with stdev. (n = 3).

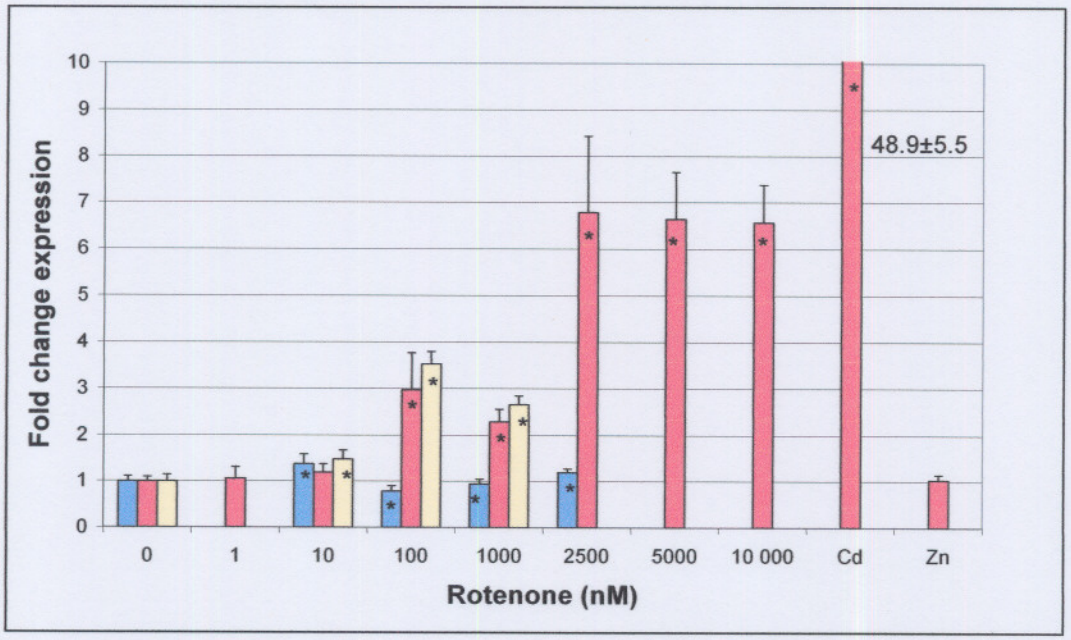

Figure 4.9: MT-IIA expression in HeLa cells treated with rotenone. Results are expressed relative to the control (0 nM rotenone) group ± stdev (n = 3). The expression of MT-2A in HeLa cells, treated with different concentrations of rotenone as well as $CdCl_2$ (12.5 μM) and $ZnCl_2$ (250 μM) is expressed (y-axis) as fold change relative to baseline expression of the control group. The incubations where performed in separate experiments over 3 (blue), 24 (red) and 48 (yellow) hours. The asterisk indicates Ct values that are statistically significant to the control group (0nM).

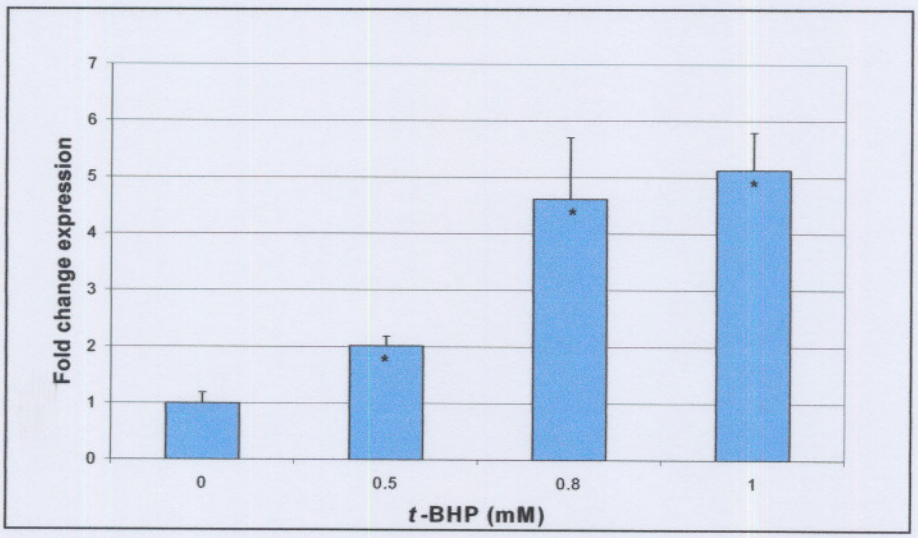

Figure 4.10: *t*-BHP induced MT-2A expression in HeLa cells. The expression of MT-2A in HeLa cells, treated with different concentrations of t-BHP is expressed (y-axis) as a fold change relative to baseline expression of the control group (0 nM rotenone) ± stdev (n = 3).

4.7 Detection of MT protein levels in HeLa cells (ELISA)

4.7.1 Optimisation of method

The competitive enzyme-linked immunosorbent assay (ELISA) essentially described by Buther *et al.* (2002) was used as a method for the determination of metallothionein protein levels in cell cultures. Several aspects of this protocol were optimised. The first change to the initial method was the use of blocking buffer (0.3% BSA, 0.05% Tween 20® in PBS) for the dilution of the detection antibody, rather than only 0.05% Tween 20® in PBS. Different dilutions of the primary and detection antibodies were investigated to determine the optimal antibody dilution. These dilutions for the primary antibody ranged from 1000 to 40 000 times in 1% Tween 20® with the detection antibody's dilution ranging between 5000 and 20 000 times in blocking buffer. During the optimisation of the antibody dilutions certain difficulties arise. It was found that repeated freeze/thawing of the antigen (MT from rabbit liver) resulted in loss of detection capability. Instability of the primary antibody was detected when stored at 4°C and the stability of the coating buffer (0.1 M $NaHCO_3$) was found to decrease when prepared and store at 4°C for more than 24 hours.

Literature suggests that when MTs are present in low levels, or small samples of tissue are available as in the case of cultured cells, the sensitivity and reproducibility required for the accurate detection of MT are lacking (Buther *et al.*, 2002). The sandwich ELISA was found to be more sensitive than the competitive method, but required two different antibodies. The availability of different MT antibodies is not as common as with other proteins, and previous researchers including Sullivan *et al.* (1998) have developed their own monoclonal or polyclonal antibodies by inoculating animals with specific antigens when measuring MT levels. The sandwich ELISA setup was tested and although different concentrations of BSA and SuperBlock®[1] reagent were used, high non-specific binding still occurred. This resulted in the

[1] SuperBlock® is a registered trademark of Pierce Biotechnology, Inc., Rockford, IL, USA.

utilisation of both monoclonal and polyclonal antibodies with the competitive ELISA method for the final analysis of MT protein levels.

Different monoclonal and polyclonal antibody dilutions were used not only to determine the best antibody to use, but also the dilution factor of the antibody. The standard range was increased in concentration (Section 3.4.2), and both antibodies initially yielded results. The monoclonal antibody was used for the rest of the optimisation of the method.

The optimisation of the sample concentration to be utilised for the detection of MT proteins had to be performed due to the non-specific binding that occurred which was not detected during the optimisation of the standard range. BSA and β-mercaptoethanol were added to samples, standards and the coating buffer to prevent non-specific binding to the plate. BSA that was added to the coating buffer prevented the colouring of the standards and samples by inhibiting the binding reaction. β-mercaptoethanol on the other hand, for an unknown reason, increased the time it took to observe a colour reaction in the standards. When BSA and β-mercaptoethanol were added only to the standards and samples, and not to the coating buffer, the time it took for the colouring reaction to occur was decreased.

A higher coating concentration was also utilised, as well as an increased blocking time of the blocking buffer, which prevented non-specific binding of the antigen to the plate. The binding capacity of the monoclonal antibody decreased due to a probable loss in stability at several times during this study which lead to the utilisation of the polyclonal antibody in the method as described in Section 3.9.2.

During the optimisation of this method, a direct ELISA method was also utilised, but due to availability of reagents, the method was not fully optimised for use in the determination of MT levels in cultured cells. The results that are presented in Section 4.7.2 are based on the competitive ELISA method as described in Section 3.9.2.

4.7.2 MT protein levels of HeLa cells treated with rotenone and *t*-BHP

Table 4.10 lists the results that were obtained for HeLa cells that were incubated with different rotenone, *t*-BHP, $CdCl_2$ and $ZnCl_2$ concentrations. Analyses of the concentration experiments were performed in triplicate and the concentrations were determined using the standard curve. The values that were obtained had a marked variation in the replicate samples. For example, the 2500 nM rotenone concentration (48 hours) varied from 0.146 – 0.548 µg MT.µg^{-1} protein as indicated in Table 4.10. The sample analyses were repeated twice resulting in values that looked the same with regard to reproducibility. These values, together with the problems encountered during the optimisation, illustrates the lack of sensitivity of this method for the determination of metallothionein levels in cell cultures. Due to these problems and cost considerations an accurate measurement of MT protein levels could unfortunately not be generated in this study. Recommendations for the measurement of MT levels are, however, discussed in Section 5.2.

Table 4.10: Data obtained for ELISA test of HeLa cells induced with rotenone and *t*-BHP

Time (hr)	Inducter (nM)	Value 1*	Value 2*	Value 3*	$Mean ± stdev
3	0	-	0.087	0.156	0.12±0.05
	10	0.056	0.060	0.119	0.08±0.04
	100	0.163	0.163	0.012	0.11±0.09
	1000	0.021	0.087	0.030	0.05±0.04
	2500	0.001	0.005	0.077	0.03±0.04
	0.5**	0.012	0.097	0.029	0.05±0.04
	0.8**	0.072	0.127	0.060	0.09±0.04
	1**	0.016	0.032	0.008	0.02±0.01
24	0	0.099	0.005	0.011	0.04±0.05
	10	0.046	0.077	0.068	0.06±0.02
	100	0.001	0.002	-	0.00±0.00
	1000	0.002	0.018	0.008	0.01±0.01
	2500	0.025	0.001	0.005	0.01±0.01
	$CdCl_2$***	0.006	0.030	0.005	0.13±0.01
	$ZnCl_2$***	0.001	0.056	0.254	0.13±0.10
48	0	0.072	0.119	0.009	0.07±0.06
	10	-	0.023	0.002	0.01±0.01
	100	0.087	0.021	0.005	0.04±0.04
	1000	0.028	0.013	0.077	0.04±0.03
	2500	0.146	0.548	0.292	0.33±0.20

*Triplicate values that are expressed as µg MT per µg protein. *** $CdCl_2$ (12.5 µM) and $ZnCl_2$ (250 µM) were included as positive controls for metallothionein expression.

CHAPTER FIVE
CONCLUSIONS

5.1 Summary and conclusions

Defects of the OXPHOS system, inherited or induced by chemicals such as rotenone, leads to alterations of various cell properties including altered ATP/ADP ratios, apoptosis, diminished antioxidant capacity and ROS production. As discussed in detail in Chapter Two, gene expression forms part of the profile of deficiencies of the OXPHOS system. Differential expression of genes in complex I deficiency has been investigated before and has revealed that MT expression could be a prominent occurrence (van der Westhuizen *et al.*, 2003). This expression profile was detected in micro-array experiments with specified conditions, and it was therefore necessary to investigate MT expression further in other experimental strategies or scenario'. It was the aim of this study to investigate a different experimental strategy via the use of an *in vitro* model (HeLa cells), treated with different concentrations of rotenone to investigate MT expression. Relevant biochemical parameters as described in Chapter Three were included in this investigation.

The conclusions made here are based on the 24 hour induction period. Investigation of the results revealed that the higher the extent of a complex I deficiency is, the higher the amount of ROS that was produced. It was demonstrated that with a complex I activity of 12.7% of baseline levels (Section 4.2.2), ROS production increased to approximately 1.8 times higher than baseline levels (Section 4.4.2) for 1000 nM rotenone. This amount of ROS increased a further 1.3 times over the next 24 hours. With total inhibition of complex I activity, results indicates a 2 time increased in ROS production with an increase of 7 times the baseline level in MT expression. Although not all MT isoforms were investigated in this study, the expression of the most ubiquitously expressed and investigated isoforms, MT-IA, -IB

and -IIA were investigated as described in Section 4.6.3.1 with only MT-IIA being induced by either rotenone or *t*-BHP in HeLa cells. This may suggest that although MT-IA and –IB was only expressed at baseline levels with rotenone and *t*-BHP induction, the induction of these two isoforms might be metal and not ROS related, since *t*-BHP and rotenone are both ROS producers. Also, the increase in MT-IIA expression with 100 nM rotenone may suggest a critical point for MT induction or the release of ROS from the mitochondria, and needs to be investigated further. HeLa cells that where induced with different concentrations of *t*-BHP, which is a direct inducer of ROS, also showed increased ROS production and MT expression of approximately 5 times compared to baseline levels. Results from other studies also indicated that MTs are induced by a variety of metals (Table 2.5) such as cadmium and zinc, which were therefore included in our study as positive controls. Results generated in this study on the other hand, indicated that only cadmium and not zinc induced MTs in complex I deficient cells as discussed in Section 4.6.3.2.

As indicated in Figure 5.1, one of the consequences of complex I deficiency is the production of ROS that leads to diminishing of the membrane potential. This was visually illustrated with the use of TMRM in Figure 4.7, where the decrease in membrane potential can clearly be observed with an increase in rotenone concentration. Furthermore, the ability of rotenone-treated cells to metabolise MTT also showed a decrease in viability although this decrease was very slow compared to the severe decrease in complex I activity. Apoptosis (caspase 3 activation) also occurs in HeLa cells with rotenone-treatment as have been reported in the study that was executed in parallel to this one (Reinecke, 2004).

From the results discussed in Chapter 4 (Section 4.4.2), it is evident that increased ROS production occurs with a complex I deficiency. Furthermore, based on what is known of the gene regulation of MTs it is likely that increased ROS levels directly induces the transcriptional response of the cells through the expression of MTs. It is therefore concluded that an induced complex I deficiency not only results in the production of ROS, but also the expression of MTs as was hypothesised in Section 2.4.1. The important question of the functional role of these proteins in complex I deficient cells is described elsewhere (Reinecke, 2004).

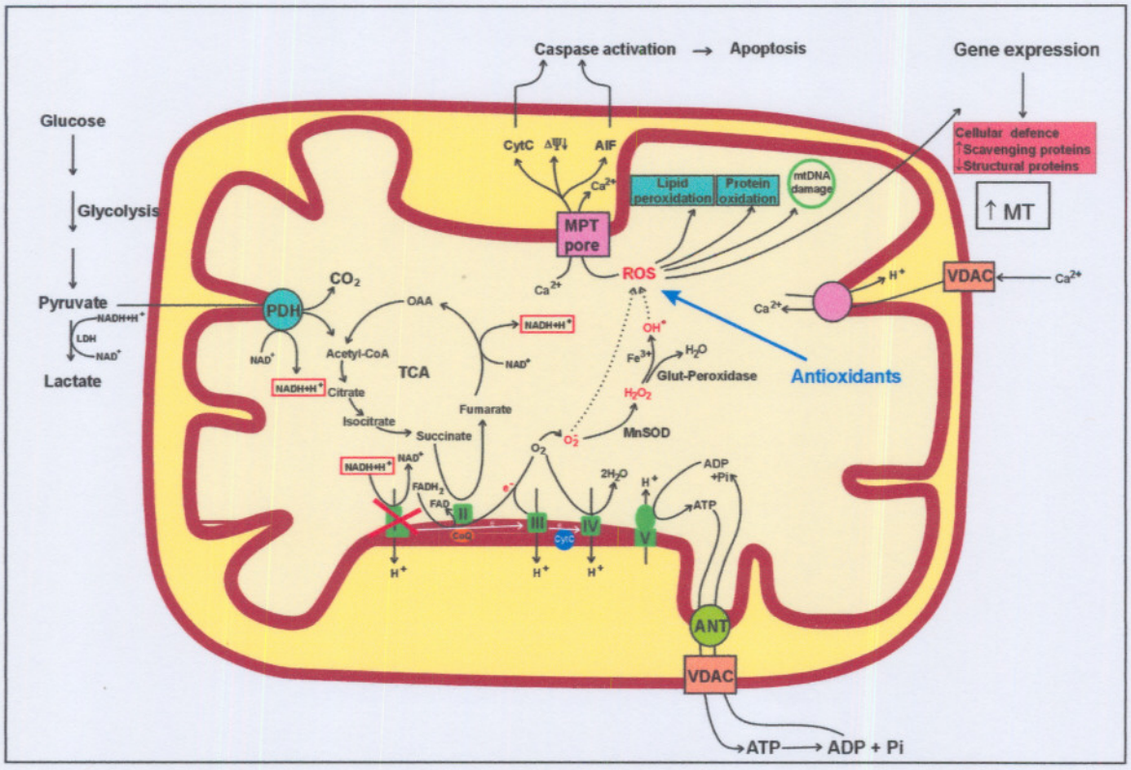

Figure 5.1: Summary of cell biological consequences of mitochondrial complex I deficiency. This Figure summarises the main metabolic functions of mitochondria that include the TCA cycle, OXPHOS system as well the antioxidant system. Under normal conditions and especially with an enzyme deficiency, e.g. complex I deficiency as indicated with the cross, the formation of ROS leads to lipid peroxidation, mtDNA damage, protein oxidation, opening of the membrane permeability pore that results in diminished membrane potential as well as the activation of apoptosis. ROS production and other trans-acting elements also affect gene expression of among other antioxidant proteins and, as indicated in this study, MT-IIA expression in HeLa cells (adapted from Wallace, 1999).

5.2 Recommendations

One of the problems experienced during this investigation was the lack of a diversity of commercially available antibodies against metallothioneins as well as the low effectivity experienced in using available antibodies to detect MTs. Although the ELISA method is one of the most sensitive immunochemical techniques available,

the reproducibility are too low. A different method is required to determine MT levels when using an *in vitro* model where only small samples and volumes are available. Some of the methods that should be investigated are Western Blots, Cd-heme affinity assays as well as lanthanide fluoroimmunoassays. Another predicament was the influence of the culture medium's pH on some of the analyses. Although precautions where taken with the seeding of the cells, it is necessary to investigate the use of other methods that are not influenced by the cell density or pH of the culture medium.

Some insights on the induction of metallothioneins were obtained, although the exact role that the different isoforms play still remains unclear. It is recommended that the different isoforms that are expressed in HeLa cells be investigated to resolve their function. Furthermore, determination of antioxidant status of cells could also shed light on the possible antioxidant role of these proteins.

REFERENCES

ANDREWS, G.K. 2000. Regulation of metallothionein gene expression by oxidative stress and metal ions. *Biochemical Pharmacology*, **59**:95-104.

ANON. 2002. [Web:] http://herkules.oulu.fi/isbn9514268490/html/i231829.html. [Date of access: 11 May 2004].

ANON. 2004a. [Web:] http://www.scripps.edu/mem/biochem/CI/overview.html. Date of access: 7 May 2004].

ANON. 2004b. [Web:] http://www.bmb.leeds.ac.uk/illingworth/oxphos/chemical.htm. [Date of access: 7 May 2004].

ANON. 2004c. [Web:] http://www.neuro.wustl.edu/neuromuscular/pathol/diagrams/mito.htm#oxphos. [Date of access: 10 May 2004].

BELOGRUDOV, G. & HATEFI, Y. 1994. Catalytic sector of complex 1 (NADH:ubiquinone oxidoreductase): subunit stoichiometry and substrate induced conformation changes. *Biochemistry*, **33**:4571-4576.

BERRIDGE, M.V., TAN, A.S., McCOY, K.D., WANG, R. 1996. Biochemical and cellular basis of cell proliferation assays that use tetrazolium salts. *Biochemica*, **4**:14-19.

BETARBET, R., SHERER, T.B., MACKENZIE, G., GARCIA-OSUNA, M., PANOV, A.V., GREENAMYRE, J.T. 2000. Chronic systemic pesticide exposure reproduces features of Parkinson's disease. *Nature Neuroscience*, **3**(12):1301-1306.

BRANDT, U., KERSCHER, S., DRÖSE, S., ZWICKER, K., ZICKERMANN, V. 2003. Proton pumping by NADH:ubiquinone oxidoreductase. A redox driven conformational change mechanism? *FEBS Letters*, **545**:9-17.

BREMNER, I. 1991. Nutritional and physiologic significance of metallothionein. *In* Methods in Enzymology, Volume **205**:25.

BUSTIN, S.A. 2000. Absolute quantification of mRNA using real-time reverse transcription polymerase chain reaction assays. *Journal of Molecular Endocrinology*, **25**:169-193.

BUTHER, H., KENNETTE, W., COLLINS, O., DEMOOR, J. KOROPATNICK, J. 2002. A Sensitive time-resolved fluorescent immunoassay for metallothionein protein. *Journal of immunological methods,* **272**:247-256.

CADENAS, E. & DAVIES, K.J.A. 2000. Mitochondrial free radical generation, oxidative stress and aging. *Free Radical Biology &* Medicine, **29**(3/4):222-230.

CHERIAN, M.G., JAYASURYA, A., BAYB, B. 2003. Metallothioneins in human tumors and potential roles in carcinogenesis. *Mutation Research*, **533**:201-209.

CHINNERY, P.F. 2000. [Web:] http://www.geneclinics.org/servlet/access?db=geneclinics&site=gt&id=8888890&key=qlSn7YjHwltVg&gry=&fcn=y&fw=K7FD&filename=/profiles/mt-overview/index.html. [Date of access: 3 August 2004].

CHINNERY, P.F. 2002. Inheritance of mitochondrial disorders. Mitochondrion, **2**:149-155.

CHOI, C. 2003. Cloning and functional study of a novel human metallothionein-1 isoform induced by paraquat. *Biochemical and Biophysical Research* Communications, **304**:236-240.

CHOMYN, A., MARTINUZZI, A., YONEDA, M., DAGA, A., HURKO, O., JOHNS, D., LAI, S.T., NONAKA, I., ANGELINI, C., ATTARDI, G. 1991. MELAS mutation in mtDNA binding site for transcription termination factor causes defects in protein synthesis and in respiration but no change in levels of upstream and downstream mature transcripts. *Proceedings of the National Science Academy of the United States of America.* **88**:10614-10618.

CHU, W.A., MOEHLENKAMP, J.D., BITTEL, D., ANDREWS, G.K., JOHNSON, J.A. 1998. Cadmium-mediated activation of the metal response element in human neuroblastoma cells lacking functional metal response element-binding transcription factor-1. *The Journal of Biological Chemistry*, **274**(9):5279-5284.

CROFTS, A. 1996. [Web:] http://www.biologie.uni-hamburg.de/b-online/library/crofts/bioph354/complex_i.html. [Date of access: 15 Augustus 2004].

CUNNINGHAM, M.L., SOLIMANB, M.S., BADRB, M.Z., MATTHEWSA, H.B. 1995. Rotenone, an anticarcinogen, inhibits cellular proliferation but not peroxisome proliferation in mouse liver. *Cancer Letters*, **95**:93-97.

DALTON, T.P., SHERTZER, H.G., PUGA, A. 1999. Regulation of gene expression by reactive oxygen. *Annual Review in Pharmacology and Toxicology*, **39**: 67-101.

DAVIES, S.R. & COUSINS, R.J. 2000. Metallothionein expression in animals: A physiological perspective on function. *Journal of Nutrition*, **130**:1085-1088.

DENIZOT, F. & LANG, R. 1986. Rapid colorimetric assay for cell growth and survival. *Journal of Immunological Methods*, **89**:271-277.

DIMAURO, S. 2000. [Web:] http://www.geneclinics.org/servlet/access?db=geneclinics&site=gt&id=8888890&key=qlSn7YjHwltVg&gry=&fcn=y&fw=5jO7&filename=/profiles/melas/index.html. [Date of access: 3 August 2004.]

DIMAURO, S. 2003. [Web:] http://www.geneclinics.org/servlet/access?id=8888890&key=qlSn7YjwltVgry= NSERGRY&fcn=y&fw=DnKM&filename=/. [Date of access: 3 August 2003].

DIMAURO, S. 2004. Mitochondrial diseases. *Biochimica et Biophysica* Acta, **1658**:80-88.

EBADI, M., IVERSENI, P.L., HAOZ, R., CERUTIS, D.R., ROJASI, I.P., HAPPE, H.K., MURRIN, L.C., PFEIFFER, R.F. 1994. Expression and regulation of brain metallothionein. *Neurochemistry International*, **27**(1):1-22.

ELMORE, S.P., NISHIMURA, Y., QIAN, T., HER,AM, B., LEMASTERS, J.J. 2004. Discrimination of depolarised from polarised mitochondria by confocal fluorescence resonance energy transfer. *Archives of Biochemistry and Biophysics.* **422**:145-152.

ESPOSTI, M.D. 1998. Inhibitors of NADH-Ubiquinone reductase: an overview. *Biochimica et Biophysica Acta*, **1364**:222-235.

GRAY, M.W., BURGER, G., LANG, B.F. 1999. Mitochondrial evolution. *Science*, **283**(5407):1476-1481.

GREENAMYRE, J.T., BETARBET, R., SHERER, T.B. 2003. The rotenone model of parkinson's disease: genes, enviroment and mitochondria. *Parkinsonism and Related Disorders*, **9**:S59-S64.

GHOSHAL, K. & JACOB, S.T. 2001. Regulation of metallothionein gene expression. *Progress in Nucleie Acid Research and Molecular Biology*, **66**:357-384.

GRIVENNIKOVA, V.G., SEREBRYANAYA, D.V., ISAKOVA, E.P., BELOZERSKAYA, T.A., VINOGRADOV, A.D. 2002. Active/de-active transition of NADH:ubiquinone oxidoreductase (Complex I) in the mitochondrial membrane of *Neurospora crassa*. *Biochemical Journal Immediate Publication*. Manuscript BJ20021165.

GRIVENNIKOVA, V.G., MAKLASHINA, E.O., GAVRIKOVA, E.V., VINOGRADOV, A.D. 1997. Interaction of the mitochondrial NADH:ubiquinone reductase with rotenone as related to the enzyme active/inactive transition. *Biochimica et Biophysica* Acta, **1319**:223-232.

HAQ, F., MAHONEY, M., KOROPATNICK, J. 2003. Signaling events for metallothionein induction. *Mutation* Research, **533**:211-226.

HAMER, D.H. 1986. Metallothionein. *Annual Review of Biochemistry*, **55**:913-951.

HAUSWIRTH, W.W. & LAIPIS, P.J. 1982. Mitochondrial DNA polymorphism in a maternal lineage of Holstein cows. *Proceedings of the National Science Academy of the United States of America*, **79**:4686-4690.

HEO, J., KIM, G.H., LEE, K.S., GO, W.U., JU, H.J., PARK, S.K., SONG, C.S., SONG, G.A., CHO, M., YANG, U.S., MOON, H.K., KIM, Y.K. 1997. Effect of Ca^{2+} channel blockers, external Ca^{2+} and phospholipase A_2 inhibitors on *t*-butylhydroperoxide-induced lipid peroxidation and toxicity in rat liver slices. *Korean Journal of Internal Medicine*, **12**(2):193-200.

HINSON, D. 2000. Rotenone characterisation and toxicity in aquatic systems. Principles of environmental toxicology. University of Idaho.

KAGI, J.H.R., HIMMELHOCH, S.R., WHANGER, P.D., BETHUNE, J.L., VALLEE, B.L. 1973. Equine hepatic and renal metallothionein. *The Journal of Biological* Chemistry, **249**(11):3537-3542.

KAGI, J.H.R. 1991. Overview of metallothioneins. *In* Methods in Enzymology, Volume **205**:614.

KARIN, M & HERSCHMANN, H.R. 1981. Induction of metallothionein in HeLa cells by dexamethasone and zinc. *European Journal of Biochemistry*, **113**(2):267-272.

KIRKINESZOS, I.G. & MORAES, C.T. 2001. Reactive oxygen species and mitochondrial diseases. *Seminars in Cell & Developmental Biology*, **12**:449-457.

KLAASENS, C.D., LIU, J., CHOUDHURI, S. 1999. Metallothionein: An intracellular protein to protect against cadmium toxicity. *Annual Review of Pharmacology and* Toxicology, **39**:267-294.

KOIZUMI, S., SONE, T., OTAKI, N., KIMURA, M. 1985. Cd2+-induced synthesis of metallothionein in HeLa cells. *Journal of Biochemistry*, **227**:879-886.

KOKOSZKA, J.E., COSKUN, P., ESPOSITO, L.A., WALLACE, D.C. 2000. Increased mitochondrial oxidative stress in the SOD2 (+/-) mouse results in the age-related decline of mitochondrial function culminating in increased apotosis. *Proceedings of the National Science Academy of the United States of America*, **98**(5):2278-2283.

LEONARD, J.V. & SCHAPIRA, H.V. 2000. Mitochondrial respiratory chain disorders I: mitochondrial DNA defects. Lancet, **355**:299-304.

McKUSICK, V.A. 2003. [Web:] http://www.ncbi.nlm.nih.gov/entrez/dispomim .cgi?id=516000#516000. [Date of access: 7 May 2004].

MENDEZ-ARMENTA, M., VILLEDA-HERNANDEZ, J., BARROSO-MOGUEL, R., NAVA-RUIZ, C., JIMENEZ-CAPDEVILLE, M.E., RIOS, C. 2003. Brain regional lipid peroxidation and metallothionein levels of developing rats exposed to cadmium and dexamethasone. *Toxicology Letters*, **144**:151-157.

MÜNGER, K., GERMANN, U.A., BELTRAMINIS, M., NIEDERMANN, D., BAITELLA-EBERLEJ, G., KAGI, J.H.R., LERCHG,K. 1985. (Cu,Zn)-Metallothioneins from fetal bovine liver. Chemical and spectroscopic properties. *The Journal of Biological* Chemistry, **260**(18):10032-10038.

MILES, A.T., HAWKSWORTH, G.M., BEATTIE, J.H., RODILLA, V. 2000. Induction, regulation, degradation, and biological significance of mammalian metallothioneins. *Critical Reviews in Biochemistry and Molecular Biology*, **35**(1):35-70.

MORIN, C. 2000. [Web:] http://members.aol.com/christofmorin/index.html. [Date of access: 10 May 2004].

OELERICH, R. 1996. [Web:] http://www.niles-hs.k12.il.us. [Date of access: 26 October 2004].

OHINISHI, T., RAGAN, C.I., HATEFI, Y. 1985. EPR studies of iron-sulfur clusters in isolated subunits and subfractions of NADH:ubiquinone oxidoreductase. *Journal of Biological Chemistry*, **260**:2782-2788.

PASSARELLA, S., ATLANTE, A., VALENTI, D., DE BARI, L. 2003. The role of mitochondrial transport in energy metabolism. *Mitochondrion,* **2**(2003):319-343.

PERKINS, G.A. & FREY, T.G. 2000. Recent structural insight into mitochondria gained by microscopy. *Micron*, **31**:97-111.

PFAFFL, M.W., HORGAN, G.W., DEMPFLE, L. 2002. Relative expression software tool (REST©) for group-wise comparison and statistical analysis of relative expression results in real-time PCR. *Nucleic Acids Research*, **30**(9):2-10.

PLUMB, J.A., MILROY, R., KAYE, S.B. 1989. Effects of the pH dependence of 3-(4,5-dimethylthiazol-2-yl)-2,5-diphenyl-tetrazolium bromide-formazan absorption on chemosensitivity determined by a novel tetrazolium-based assay. *Cancer Research.* **49**(16):4435-4440.

RADONIC, A., THULKE, S., MACKAY, I.M., LANDT, O., SIEGERT, W., NITSCHE, A., 2004. Guideline to reference gene selection for quantitative real-time PCR. *Biochem. Biophys. Res. Commun.* **313**, 856-862.

RAHMAN, S., BLOK, R.B., DAHL, H.H., DANKS, D.M., KIRBY, D.M., CHOW, C.W., CHRISTODOULOU, J., THORBURN, D.R. 1996. Leigh syndrome: clinical features and biochemical and DNA abnormalities. *Annual Neurology.* **39**(3):343-351.

REINECKE, F. 2004. Functional properties of metallothionein overexpression in NADH:ubiquinone oxidoreductase deficiency in HeLa cells. Potchefstroom : North-West University. (Dissertation – M.Sc.)

ROZEN, S. & SKALETSKY, H.J. 2000. Primer3 on the WWW for general users and for biologist programmers. In: Krawetz S, Misener S (eds) *Bioinformatics Methods and Protocols: Methods in Molecular Biology.* Humana Press, Totowa, NJ, 365-386.

SATO, M. & BREMNER, I. 1993. Oxygen free radical and metallothionein. *Free Radical Biological and Medicine*, **14**:325-337.

SATO, M. & KONDOH, M. 2002. Recent studies on metallothionein: Protection against toxicity of heavy metals and oxygen free radicals. *Tohoku Journal of Experimental Medicine*, **196**:9-22.

SCHEFFLER, I.E. 2001. A century of mitochondrial research: achievements and perspectives. *Mitochondrion*, **1**:3-31.

SMEITINK, J.A.M., LOEFFEN, J.L.C.M., TRIEPELS, R.H., SMEETS, R.J.P., TRIJBELS, M.F., VAN DEN HEUVEL, L.P. 1998. Nuclear genes of human complex 1 of the mitochondrial electron transport chain: state of the art. *Human Molecular* Genetics, **7**(10):1573-1579.

SMEITINK, J.A.M., VAN DEN HEUVEL, L.W.P.J., DIMAURO, S. 2001. The genetics and pathology of oxidative phosphorylation. *Nature Review of Genetics*, **2**:342-352.

SMEITINK, J.A.M., VAN DEN HEUVEL, L.W.P.J., KOOPMAN, W.J.H., NIJTMANS, L.G.J. 2004. Cell biological consequences of mitochondrial NADH:Ubiquinone oxidoreductase deficiency. *Current Neurovascular Research,* **1**(1): 1-12.

STENNARD, F.A., HOLLOWAY, A.F. HAMILTON, J., WEST, A.K. 1993. Characterisation of six additional metallothionein genes. *Biochimica et Biophysica Acta*, **1218**:357-365.

STOSCHECK, C.M. 1990. Quantitation of Protein. *In* Methods in Enzymology, Volume **182**:50-68.

SULLIVAN, V.K., BURNETT, F.R., COUSINS, R.J. 1998. Metallothionein expression is increased in monocytes and erythrocytes of young men during zinc supplementation. *Nutrition.* **128**: 707-713.

THOMAS, J. A. 1999. Oxidative stress including glutathione, a peptide for cellular defence against oxidative stress. Department of Biochemistry and Biophysics, Iowa state University, 1-10.

TROUNCE, I.A., KIM, Y.L., JUN, A.S., WALLACE, D.C. 1996. Assessment of mitochondrial oxidative phosphorylation in patient muscle biopsies, lymphoblasts, and transmitochondrial cell lines. *In* Methods in Enzymology, Volume **264**: 484-509.

VANDESOPMPELE, J., DE PRETER, K., PATTYN, F., POPPE, B., VAN ROY, N., DE PAEPE, A., SPELEMAN, F. 2002. Accurate normalization of real-time quantitative RT-PCR data by geometric averaging of multiple internal control genes. *Genome Biology*, **3**(7):0034.1-0034.11

VAN DER WESTHUIZEN, F.H., VAN DEN HEUVEL, L.P., SMEETS, R., VELTMAN, J.A., PFUNDT, R., VAN KESSEL, A.G., URSING, B.M., SMEITINK, J.A.M. 2003. Human mitochondrial complex I deficiency: Investigating transcriptional responses by microarray. *Neuropediatrics*, **34**:14-22.

VOET, D. & VOET, J.G. 1995. Biochemistry. 2nd Edition. New York : Wiley. 6.

WANG, H. & JOSEPH, J.A. 1999. Quantifying cellular oxidative stress by dichorofluorescein assay using microplate reader. *Free Radical Biology and Medicine*, **27**(5/6):612-616.

WILSON, J. & WALKER, K. 1994. Practical biochemistry: Principles and techniques. 4th Edition. Cambridge University Press : Cambridge. 95-99.

WALLACE, D.C. 1999. Mitochondrial disease in man and mouse. *Science*, **283**:1482-1488.

WALLACE, D.C., SINGH, G., LOTT, M.T., HODGE, J.A., SCHURR, T.G., LEZZA, A.M., ELSAS, L.J., NIKOSKELAINEN, E.K. 1988. Mitochondrial DNA mutation associated with Leber's Hereditary Optic Neuropathy. *Science*, **242**:1427-1430.

YURKOW, E.J. & DECOSTE, C.J. 1999. Effects of cadmium on metallothionein levels in human peripheral blood leukocytes: a comparison with zinc. *Journal of Toxicology and Environmental Health.* **58**(5):313-27.

ZHANG, B., GEORGIEV, O., HAGMANN, M., GÜNES, A., CRAMER, M., FALLER, P. 2003. Activity of metal-responsive transcription factor 1 by toxic heavy metals and H_2O_2 in vitro is modulated by metallothionein. *Molecular and Cellular* Biology, **23**(23):8471-8485.

APPENDIX A

Validation of housekeeping genes suitability as normalization controls in rotenone-induced Complex I deficient HeLa cells

Oksana Levanets[a], Antonel Olckers[b], Francois H. van der Westhuizen[a,*]

[a]Division of Biochemistry, School for Chemistry and Biochemistry, North-West University, Potchefstroom, South Africa

[b]Center for Genome Research, North-West University, Pretoria, South Africa

*Corresponding author: [a]Division of Biochemistry, School for Chemistry and Biochemistry, North-West University, Hoffmanstreet, Potchefstroom, 2520, South Africa. Tel: +27 18 2992318, Fax +27 18 2992316, E-mail: bchfhvdw@puk.ac.za

Abstract

The contribution of transcriptional responses to the cellular consequences in mitochondrial disease has clearly become evident in recent years. One of the tools to investigate these responses, quantitative real-time PCR (RT-PCR) is regarded as one of the most reliable and rapid methods but requires reference genes for normalization. We evaluated the expression variation of five commonly used housekeeping genes in rotenone-induced complex I deficient HeLa cells. 18S rRNA was found to be the most stable gene, followed by β-microglobulin, GAPDH, β-actin and RNA polymerase II. Although the selection of housekeeping genes for the normalization of expression data depends on the specific experimental conditions and cell line, these results may by useful for selecting suitable housekeeping genes when investigating transcriptional responses in mitochondrial deficiencies.

Keywords: *Quantitative real-time PCR; Reference genes; Housekeeping genes; Transcription analysis; Mitochondrial complex I deficiency; Rotenone.*

1. Introduction

The cell biological consequences of deficiencies of the oxidative phosphorylation (OXPHOS) system are complex and include a diversity of cellular processes such as metabolic and signal transduction imbalances as well as oxidative stress-related damage (Briére *et al.*, 2004). The disease expression depends on several factors, including the genotype and tissues affected. Much interest currently exists in the contribution of mitochondrial and nuclear transcriptional responses to the phenotype expression of mitochondria-related diseases, of which NADH:ubiquinone oxidoreductase (complex I) deficiency is one of the most frequently encountered (Triepels *et al.*, 2001; Loeffen *et al.*, 2000). Although limited data still exists, it is becoming evident that nuclear-mitochondrial communication may play a distinct role in the pathology of the complex I deficiency (van der Westhuizen *et al.*, 2003; Heddi *et al.*, 1999; Collombet *et al.*, 1997).

For the investigation of transcriptional responses many techniques allow quantitative analysis of mRNA expression such as Northern blotting, *in situ* hybridization, RNase protection, microarray analysis and competitive RT-PCR. Quantitative real-time PCR has become a powerful tool for transcription quantification in recent years due to its high accuracy, broad dynamic range, and sensitivity. Independent of the techniques used, quantifications are generally normalized using so-called housekeeping genes as invariant controls to account for sample handling, loading and experimental variation. This practice is being questioned as it becomes increasingly clear that some housekeeping genes may vary considerably in certain biological samples (Bustin, 2002). Therefore, identifying suitable control genes has become one of the important problems in such investigations. To assist these types of studies we investigated the stability of expression of certain commonly used housekeeping genes, including glyceraldehyde-3-phosphate dehydrogenase (GAPDH), β-actin, β-2-microglobulin (β-2-MG), RNA polymerase II (RP2) and 18S rRNA, in rotenone-induced complex I-deficient HeLa cells.

2. Materials and methods

2.1. Cell culture and rotenone treatments

HeLa cells were cultured in Dulbecco's Modified Eagles medium (DMEM) containing 5% (v/v) fetal calf serum and antibiotics (penicillin, 250U/ml; streptomycin, 250µg/ml) in a humidified incubator at 37 °C and 5% CO_2. To cultures that were approximately 70% confluent in 25 cm^2-flasks rotenone was added at various final concentrations ranging between 0 and 10 µM. These incubations enabled the induction of complex I deficient cell lines with rotenone-sensitive residual enzyme activities of approximately 100% (at 0 nM rotenone), 50% (10 nM), 30% (100 nM), 12% (1000 nM) and 0% (2.5 µM and higher), as measured in enriched mitochondrial preparations and normalized against citrate synthase activity (Rahman *et al.*, 1996). As a control for the induction of oxidative stress, *tert*-butyl hydroperoxide (*t*-BHP) at concentrations ranging between 0.5 and 1.0 mM were included in the array of incubations. Separate sets of incubations were performed for 24 and 48 hours.

2.3. RNA isolation and cDNA synthesis

Total RNA was isolated using QIAzol™ reagent (Qiagen, Hilden, Germany) according to instructions and the RNA integrity was electrophoretically verified by ethidium bromide staining. 3 µg of RNA was reverse transcribed with 200U M-MLV Reverse Transcriptase (Promega, Madison, WI) in a volume of 40 µl using 0.5 µg random hexamer primers (Promega) according to manufacturer's instructions.

2.4. Quantitative real-time PCR

The sequences of all primers used for the PCR are listed in Table 1. Real-time quantitative PCR was performed using an iCycler iQ™ (Bio-Rad, Hercules, CA) in a final volume of 20 µl using the SYBR Green method. The PCR reaction consisted of 10 µl iQ™ SYBR® Green Supermix (Bio-Rad, Hercules, CA), 500 nM of forward and reverse primers, and 75 ng of cDNA (3 ng for 18S rRNA primers). A four-step experimental run protocol was used: 1) initial denaturation (3 min. at 95 °C); 2) 35 cycles of denaturation at 95 °C for 20 sec, primer annealing at 60 °C for 10 sec,

extension at 72 °C for 20 sec and an additional step at 82 °C (84 °C for 18S rRNA primers) with a single fluorescense measurement; 3) final extension at 72 °C for 5 min; 4) melting curve analysis (55-95 °C with a heating rate of 0.5 °C per 5 sec and fluorescent measurement every 5 sec). A high temperature fluorescence measurement point at the end of the fourth segment was performed to improve SYBR Green quantification (Pfaffl *et al.*, 2002). Fluorescence was measured following each cycle and displayed graphically (iCycler iQ Real-time Detection System Software, version 3.0, BioRad, Hercules, CA). The software determined a cycle threshold (Ct) value, which identified the number of PCR cycles where the fluorescence signal exceeds the detection threshold value for that sample. This threshold is set to the log linear range of the amplification curve and kept constant for data analysis throughout the study. Every assay included a no-template control, five serial dilution points (in steps of 5-fold) of a cDNA mixture, as well as each of the test cDNA's. All samples were amplified in triplicates and the mean value was used for further calculations.

2.5. Calculations and statistical analysis

Results (Ct values) from iCycler iQ Real-time Detection System were analyzed by Statistica Version 6.1 software (StatSoft, Tulsa, OK) and BestKeeper software tool (Pfaffl *et al.*, 2004). PCR efficiency for each primer set was calculated by serial dilutions method using REST software tool (Pfaffl *et al.*, 2002). The relative expression quantities for each sample were calculated by the comparative Ct method and gene expression stability was analyzed using GeNorm software tool (Vandesompele *et al.*, 2002).

3. Results

Quantitative real-time RT-PCR was performed on total RNA samples obtained from HeLa cells that were treated with various rotenone concentrations, resulting in residual complex I activities ranging between 0 and 100%, as well as *t*-BHP-induced oxidative stress. To ensure comparability between the analyses of all five housekeeping genes, we first determined the reaction efficiency of each individual assay by measuring serial dilutions of 75 ng cDNA in triplicate (Pfaffl *et al.*, 2002). All

PCR reactions displayed efficiency between 88% and 100%. The variations in the cycle threshold (Ct) values, which represent the cycle where a significant increase in amount of PCR product occurs, are summarized in Figure 1. Comparing the median expression values (Ct values) of the housekeeping genes, as shown in Figure 1, the variability for housekeeping gene expression was clearly less in the case of the 18S rRNA as compared to the other genes. Ct values were also expressed as relative expression quantities and analyzed using the GeNorm software tool. The results of this analysis are presented as GeNorm expression stability values (or gene stability measures, M), which are defined as average pairwise variations of a particular gene with all other control genes as summarized in Table 2 (Vandesompele *et al.*, 2002). Genes with the lowest M values have the most stable expression. Figure 2 shows the standard deviation expressed as a fold change from the mean and range expressed as maximum variability for housekeeping genes after rotenone treatment. The most stable housekeeping gene in these conditions was 18S rRNA with a maximum variability of 1.3 fold change. The most variable genes were RNA polymerase II and β-actin (1.97 and 1.96 fold change, respectively).

4. Discussion

One of the essential consequences of mitochondrial disease is altered expression of some genes involved in bioenergetics (van der Westhuizen *et al.*, 2003; Heddi *et al.*, 1999; Collombet *et al.*, 1997). Investigations of transcriptional responses will no doubt contribute to our understanding of the disease and with the tools currently available present exciting challenges. Real-time PCR is one of the most accurate and commonly used methods to evaluate changes in gene expression. A parallel quantification of a housekeeping gene is a commonly used approach for the validation of the expression of tested gene. The first comparisons of the levels of gene expression were based on the assumption that constant expression of housekeeping genes exist in all the tissues and cells under all conditions. But it became clear that various incubating conditions and different stress or pathological states of the organism strongly influence the expression of housekeeping genes (Thellin *et al.*, 1999; Bustin, 2002; Radonic *et al.*, 2004). To avoid these problems evaluating expression stability of several housekeeping genes under the

experimental conditions should be performed before selecting the most stable gene or a panel of genes for normalization (Bustin, 2002).

To define suitable internal controls for gene expression quantification in an *in vitro* complex I deficient model we titrated HeLa cells with rotenone. *In vitro* modulation of mitochondrial electron transport is often used to investigate underlying mechanisms of these diseases (Mojet *et al.*, 1997; Luetjens *et al.*, 2000; Chinopoulos and Adam-Vizi, 2001). Rotenone is commonly used specific and irreversible inhibitor of complex I have been shown to induce apoptosis via the production of reactive oxygen species in several cell lines (Li *et al.*, 2003). For analysis of housekeeping genes expression stability we have chosen commonly used genes representing different biological activities including glycolysis, cytoskeleton structure and kinetics, immune response, gene expression and protein biosynthesis. Our study of internal controls stability in conditions of induced mitochondrial complex I deficiency revealed 18S rRNA to be the most stable and most suitable for normalization of tested genes expression quantification both for 24 and 48 h treatments. The maximum fold change in expression level for 18S rRNA under conditions where low to high levels of complex 1 activity, oxidative stress and apoptosis occur was only 1.3 times. Using 18S rRNA as an internal control, however, has some disadvantages. Firstly, it's possible to use only total RNA for quantification and to synthesize cDNA with random primers. Secondly, 18S rRNA gene contains no introns and transcript amplification therefore is susceptible to false results from contaminating DNA. And thirdly, due to the high abundance of rRNA transcripts, using 18S rRNA as an internal control for studies of genes expressed at relatively low levels requires additional dilution of cDNA templates or lower primer concentrations for its amplification. As expected, 18S rRNA was the most abundant of transcripts (lowest Ct value even after 25 times cDNA dilution), and RNA polymerase II transcript appeared to be the least abundant.

RNA polymerase II and β-actin appeared to be the most variable in our experimental conditions, but even for these genes expression variability levels (maximum 1.97 and 1.96 fold changes, respectively) allow use them for normalization in quantification experiments.

In conclusion, according to our data, the rank of housekeeping genes expression stability in conditions of rotenone-induced complex I deficient HeLa cells is 18S rRNA, β-microglobulin, GAPDH, β-actin, RNA polymerase II. As none of the genes has transcription variation of more than two all of these genes should be suitable as internal controls in similar experiments. However, each of these genes has some advantages and disadvantages as internal controls which must be considered. Although current opinion suggests the preferable use of a housekeeping gene panel for obtaining more accurate results in quantification, we believe our data could be useful when considering a normalization strategy for investigations of transcriptional responses in mitochondrial disease.

Acknowledgements

The authors would like to thank the National Research Foundation of South Africa for financial support (GUN 2053704). We would also like to thank the staff of the School of Pharmacy, North-West University, for use of PCR apparatus and the staff of the Mitochondrial Research Laboratory, North-West University, for assistance.

References

Bustin, S.A., 2002. Quantification of mRNA using real-time reverse transcription PCR (RT-PCR): trends and problems. J. Mol. Endocrinol. 29, 23-39.

Brière, J.J., Chrétien, D., Bénit, P., Rustin, P., 2004. Respiratory chain defects: what do we know for sure about their consequences in vivo? Biochimica et Biophysica Acta (BBA) – Bioenergetics In Press.

Chinopoulos, C., Adam-Vizi, V., 2001. Mitochondria deficient in complex I activity are depolarized by hydrogen peroxide in nerve terminals: Relevance to Parkinson's disease. J. Neurochem. 76, 302-306.

Collombet, J.M., Faure-Vigny, H., Mandon, G., Dumoulin, R., Boissier, S., Bernard, A., Mousson, B., Stepien, G., 1997. Expression of oxidative phosphorylation genes in muscle cell cultures from patients with mitochondrial myopathies. Mol. Cell. Biochem. 168, 73-85.

Heddi, A., Stepien, G., Benke, P.J., Wallace, D.C., 1999. Coordinate induction of gene expression in tissues of mitochondrial disease. J. Biol. Chem. 274, 22968-22976.

Li, N., Ragheb, K., Lawler, G., Sturgis, J., Rajwa, B., Melendez, J.A., Robinson, J.P., 2003. Mitochondrial complex I inhibitor rotenone induces apoptosis through

enhancing mitochondrial reactive oxygen species production. J. Biol. Chem. 278, 8516-8525.

Loeffen, J.L., Smeitink, J.A., Trijbels, J.M., Janssen, A.J., Triepels, R.H., Sengers, R.C., van den Heuvel, L.P., 2000. Isolated complex I deficiency in children: clinical, biochemical and genetic aspects. Hum. Mutat. 15, 123-34.

Luetjens, C.M., Bul, N.T., Sengpiel, B., Munstermann, G., Poppe, M., Krohn, A.J., Bauerbach, E., Kriegstein, J., Prehn, J.H., 2000. Delayed mitochondrial disfunction in excitotoxic neuron death: Cytochrome *c* release and a secondary increase in superoxide production. J. Neurosci. 20, 5715-5723.

Mojet, M.H., Mills, E., Duchen, M.R., 1997. Hypoxia-induced catecholamine secretion in isolated newborn rat adrenal chromaffin cells is mimicked by inhibition of mitochondrial respiration. J. Physiol. 504, 175-189.

Pfaffl, M.W., Horgan, G.W., Dempfle, L., 2002. Relative expression software tool (REST) for group-wise comparison and statistical analysis of relative expression results in real-time PCR. Nucleic Acids Res. 30, e36.

Pfaffl, M.W., Tichopad, A., Prgomet, C., Neuvians, T.P., 2004. Determination of stable housekeeping genes, differentially regulated target genes and sample integrity: BestKeeper--Excel-based tool using pair-wise correlations. Biotechnol. Lett. 26, 509-515.

Rahman, S., Blok, R.B., Dahl, H.H., Danks, D.M., Kirby, D.M., Chow, C.W., Christodoulou, J., Thorburn, D.R., 1996. Leigh syndrome: clinical features and biochemical and DNA abnormalities. Ann. Neurol. 39, 343–351.

Radonic, A., Thulke, S., Mackay, I.M., Landt, O., Siegert, W., Nitsche, A., 2004. Guideline to reference gene selection for quantitative real-time PCR. Biochem. Biophys. Res. Commun. 313, 856-862.

Thellin, O., Zorzi, W., Lakaye, B., De Borman, B., Coumans, B., Hennen, G., Grisar, T., Igout, A., Heinen, E., 1999. Housekeeping genes as internal standards: use and limits. J. Biotechnol. 75, 291-295.

Triepels, R.H., van den Heuvel, L.P., Trijbels, J.M., Smeitink, J.A., 2001. Respiratory chain complex I deficiency. Am. J. Med. Genet. 106, 37-45.

van der Westhuizen, F.H., van den Heuvel, L.P., Smeets, R., Veltman, J.A., Pfundt, R., van Kessel, A.G., Ursing, B.M., Smeitink, J.A., 2003. Human mitochondrial complex I deficiency: investigating transcriptional responses by microarray. Neuropediatrics 34, 14-22.

Vandesompele, J., De Preter, K., Pattyn, F., Poppe, B., Van Roy, N., De Paepe, A., Speleman, F., 2002. Accurate normalization of real-time quantitative RT-PCR data by geometric averaging of multiple internal control genes. Genome Biol. 3, research0034.1–research0034.11.

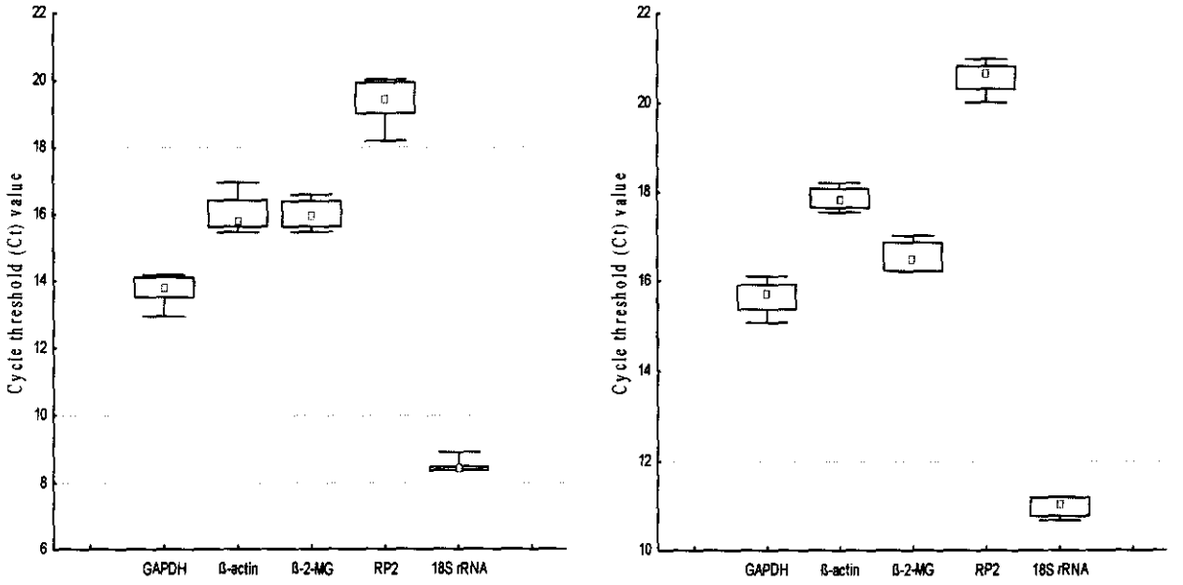

Fig. 1. The RNA transcription levels of the tested housekeeping genes in absolute Ct values in conditions of rotenone-induced complex I deficiency in HeLa cells (A, 24 h induction; B, 48 h induction). The median values are indicated by small squares, 25 - 75% percentiles are indicated by the boxes and minimum and maximum values indicated by whiskers.

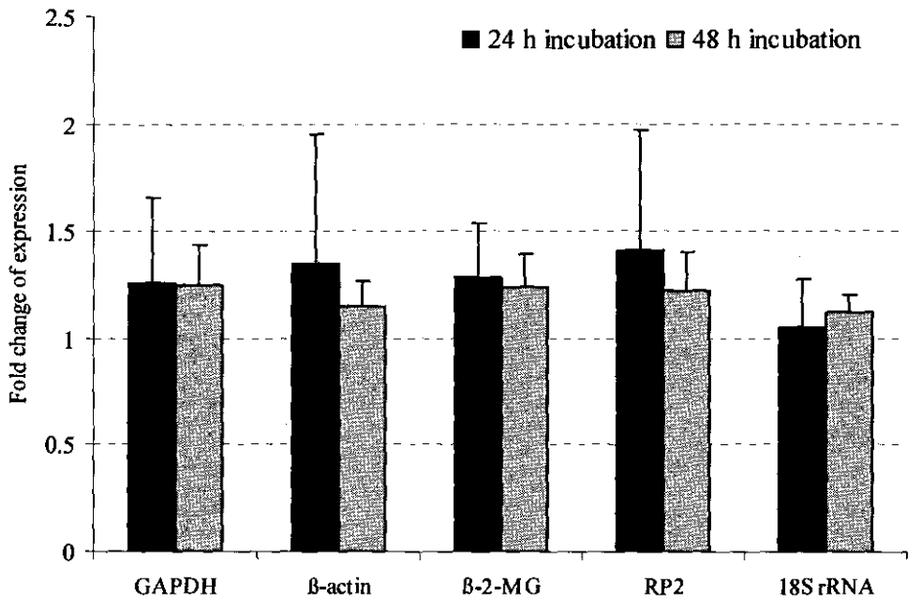

Fig. 2. Changes in housekeeping genes expression in rotenone-induced complex I deficient HeLa cells. Variability of genes expression shown as an average fold change from the mean (columns) and maximum fold change (error bars).

Table 1: Gene specific primers used for real-time PCR.

Gene	Primers	Sequence	Accession number	Reference	Amplicon size, bp
GAPDH	GAPDH-Fwd GAPDH-Rev	GAAGGTGAAGGTCGGAGTC GAAGATGGTGATGGGATTTC	NM_002046	Radonic *et al.*, 2004	226
β-actin	Beta-Act-Fwd Beta-Act-Rev	AGCCTCGCCTTTGCCGA CTGGTGCCTGGGGCG	NM_001101	Radonic *et al.*, 2004	174
β-2-microglobulin	Beta-2-MG-Fwd Beta-2-MG-Rev	AGCGTACTCCAAAGATTCAGGTT ATGATGCTGCTTACATGTCTCGAT	NM_004048	Radonic *et al.*, 2004	306
RNA polymerase II	RP2-Fwd RP2-Rev	GCACCACGTCCAATGACAT GTGCGGCTGCTTCCATAA	X63564	Radonic *et al.*, 2004	267
18S rRNA	18SrRNA-Fwd 18SrRNA-Rev	GTGCATGGCCGTTCTTAGTT CGGACATCTAAGGGCATCAC	X03205	Generated by Primer3 software	187

Table 2: GeNorm analysis of housekeeping genes expression stability.

Gene	M (24 h)	M (48 h)
18S rRNA	0.466	0.402
Beta-2-microglobulin	0.548	0.503
GAPDH	0.575	0.506
Beta-actin	0.682	0.512
RNA polymerase II	0.730	0.532

Results are shown as GeNorm expression stability values or M, the internal control gene-stability measure, defined as average pairwise variation of a particular gene with all other control genes (Vandesompele *et al.*, 2002). Genes with the lowest M values have the most stable expression.